Advanced Detection Strategies for Ultrasound Contrast Agents

ISBN 90-9018845-2

Cover design by Universal Press.

Advanced Detection Strategies for Ultrasound Contrast Agents

Geavanceerde detectiemethoden voor ultrageluidscontrastmiddelen

Proefschrift

ter verkrijging van de graad van doctor aan de
Erasmus Universiteit Rotterdam
op gezag van de
Rector Magnificus

Prof.dr. S.W.J. Lamberts

en volgens besluit van het College voor Promoties.
De openbare verdediging zal plaatsvinden op

woensdag 19 januari 2005 om 15.45 uur
door

Jerome Maria George Borsboom
geboren te Rotterdam

Promotiecommissie

Promotoren:	Prof.dr.ir. N. de Jong Prof.dr.ir. A.F.W. van der Steen
Overige leden:	Prof.dr. D.J.G.M Duncker Prof.dr. H.G. Torp Prof.dr. Y. Takeuchi

This work has been supported by the Technology Foundation STW (RKG-5104) and the Interuniversity Cardiology Institute of the Netherlands (ICIN).

Financial support by Oldelft Ultrasonics BV and Bracco Research SA is gratefully acknowledged.

"If we, citizens, do not support our artists, then we sacrifice our imagination on the altar of crude reality and we end up believing in nothing and having worthless dreams."

Yann Martel, author of 'Life of Pi'

CONTENTS

1 GENERAL INTRODUCTION

1.1 CONTRAST AGENTS

Ultrasound contrast agent was discovered serendipitously by Gramiak and Shah[22] in 1968 when they injected indocyanine green dye into the heart and observed increased echogenicity of the blood containing the dye. Small cavitation bubbles that were formed upon injection of the dye were traced to be the source of the enhanced echoes[23]. Nowadays, ultrasound contrast agent still consists of small bubbles that are free flowing in the blood stream. However, as the uncontrolled process of cavitation and violent collapse is considered harmful for cells and tissue, contrast agent is usually prepared under controlled conditions outside the body and injected through a vein where they are taken up into the blood stream and transported to the region under investigation[1].

Current contrast agents consist of small (1–10 μm diameter) encapsulated gas filled micro-spheres with well defined properties and size distribution. Their sizes are small enough to enable them to pass the lung circulation and reach the left ventricle, and prevent possibly harmful emboli formation. Encapsulation is necessary to prevent rapid dissolution of the gas content into the blood[5]. Although the newest agents employ gasses that have low blood solubility like SF_6 and C_4F_{10} which lengthen the lifetime of a free gas bubble into the 100-millisecond range, this is not enough, though, to cover the travelling time from site of injection to the site of interest.

On insonification with ultrasound, a contrast agent bubble starts to oscillate under the pressure of the sound field. This oscillating behaviour is the primary source of the high scattering strength of the agent[24]. Therefore, a lot of research has been focussed on the development of a model describing the oscillations of a bubble as a function of the incident sound wave. Among others, de Jong[15], Frinking[19], Church[11] and Morgan[32] each have proposed a differential equation that describes bubble wall excursions as a function of the incident pressure. The main difference between the equations is the way the shell and its properties are represented. As the exact properties and layout of the bubble shell are generally not well understood, some amount of ad-hoc reasoning was put into the development of these bubble models. Recently, however, the application of very high frame rate cameras made it possible to observe the oscillations of a contrast agent bubble optically[10, 34]. This development greatly

enhances the possibility to study a single bubble experimentally which will eventually lead to more accurate bubble models and a better understanding of the behaviour of contrast agent.

1.2 DETECTION METHODS

The usability of the contrast agent is very dependent on the ability to detect the presence of the agent in blood or tissue. On injection, ultrasound contrast agent mixes with the blood and is transported to the region of interest where it can enhance the quality of the image. For hypo-echoic regions like the cavities of the human heart, the high scattering strength of contrast agents can be used for detection. However, when the agent is in the capillaries and surrounded by tissue detection will be more difficult as the echo from a contrast bubble will be confounded with the echo from the surrounding tissue. In addition, the number of contrast agent bubbles in the capillaries will be low, further decreasing its detectability. By developing specially tailored signal processing methods, we attempt to separate the reflections from contrast bubbles and the surrounding tissue and hence improve the visibility of the areas where contrast agent is present.

Initially, the high scattering power of contrast agent bubbles was used to detect the presence of contrast agent. For example, the delineation of the left ventricle was significantly improved by the increase of image intensity when using ultrasound contrast agents. However, for detection of contrast agent in tissues, new detection methods had to be developed. These methods can be roughly divided into two categories. Detection of contrast agent is either based on separation of the echoes from the agent and the surrounding tissue or on destruction of the contrast agent. The former category is purely signature based and includes techniques like harmonic imaging[38], pulse inversion[25], power modulation[7], subharmonic imaging[17], super-harmonic imaging[4, 6] and ultra-harmonic imaging[40]. These techniques use a spectral filtering approach to separate the contribution from tissue and contrast agent. As these techniques often exploit the strong non-linear characteristics of a contrast bubble, development of these techniques coincided with the development of tissue harmonic imaging techniques. The latter category is based on temporal differences in signature and includes techniques like release burst imaging[18] and in general all contrast imaging methods that operate at high ultrasound pressures (MI>0.1). The following describe some of the important contrast agent detection methods currently in use. Special consideration will be given to the performance of these techniques in terms of SNR and CTR gain.

HARMONIC IMAGING

The first technique to be based on the harmonic response of contrast agent is harmonic imaging[38]. Development of the technique coincided with the advent of tissue

harmonic imaging which uses harmonics generated by non-linear propagation. To exploit the high level of harmonics reflected by a contrast agent bubble, the echo signal is filtered with a band-pass filter to extract the second harmonic from the response. Using the second harmonic, a much larger difference between tissue echo levels and contrast agent echo levels is found than when using the fundamental. Compared to the CTR at the fundamental, harmonics imaging will significantly improve the CTR. However, for fair evaluation of the detection technique, the CTR before and after processing should be compared at the frequencies where the technique operates. For harmonic imaging this implies that the CTR does not change after processing as the only processing consists of filtering which does not change the relative levels at each frequency. Neither does the SNR improve. However, compared to the multi-pulse techniques discussed below, this technique does not suffer from motion artefacts or reduced frame rate.

PULSE INVERSION

One of the techniques that use cancellation of spectral parts of the response is pulse inversion[25]. Based on cancellation of the odd functions in a power expansion of the response, it suppresses the odd harmonics and hence improves the discrimination of contrast agent and tissue. In its simplest form, pulse inversion is a two pulse technique in which a regular broadband ultrasound pulse and a phase inverted copy of this pulse are alternately sent into the medium. For every pair of received echoes, the echo resulting from the phase inverted pulse is added to the echo from the not phase inverted excitation. For linear systems the result is full cancellation of the responses as both echoes are equal except for the phase inversion. However, due to non-linear effects in the propagation of the pulse through the medium and in the response a contrast agent bubbles, the received echo will contain frequencies that were not present in the excitation signal. With pulse inversion part of these frequencies will be suppressed in favour of frequencies that show better discrimination of contrast agent and tissue. The pulse inversion method using two pulses has been extended to use more than two pulses. Wilkening[45] has proposed a number of pulsing schemes with more than two pulses with phase shifts other than 180 degrees. These pulsing schemes can suppress other harmonics than the even harmonics that are suppressed with the regular two pulse scheme. A disadvantage of the pulse inversion techniques is its susceptibility to motion artefacts. However, with the high pulse repetition frequencies that are currently in use, these artefacts are not a major concern.

The basic operating principle of pulse inversion for contrast agent detection is the suppression of the odd harmonics in the response. As the non-linearity of a contrast agent bubble at non-destructive imaging pressure levels is in general much higher than the non-linearity of the surrounding tissue, detection with pulse inversion is fully based on the relative levels of second harmonic in the received echo. Hence, the CTR at the second harmonic that is present in the unprocessed echoes does not increase with pulse inversion and might even slightly decrease as the response of a contrast agent bubble

cannot be very accurately represented with a power series expansion. The addition step in pulse inversion essentially amounts to averaging the two traces with appropriate gain factors. Therefore, pulse inversion, in theory, improves the SNR with 3 dB.

POWER MODULATION

Power modulation is another technique that suppresses spectral part of the response[7]. Based on the scaling property of linearity, power modulation cancels the linear echoes from the response to obtain a response purely based on harmonic echoes. As with harmonic imaging, this improves the quality of the image due to the high non-linear scattering strength of contrast agent. Power modulation operates by sending two pulses into the medium which are equal in pulse shape, but have different amplitudes. For every pair of received echoes, the resulting echoes are scaled according to the inverse of the sending amplitude and, subsequently, the first echo is subtracted from the second echo. As with pulse inversion, for linear systems the result is full cancellation of the responses as both echoes are equal except for the amplitude difference. However, due to non-linear effects in the propagation of the pulse through the medium and in the response a contrast agent bubbles, the received echo will contain frequencies that were not present in the excitation signal. As the generation of harmonics is dependent on the amplitude of the excitation, the higher amplitude pulse will have generated more harmonics than the low amplitude pulse relative to the fundamental. Therefore, the subtraction will not fully suppress the harmonics in the response. In contrast to pulse inversion, only the fundamental will be highly suppressed. Therefore, the remaining signal will contain odd and even harmonics.

Evaluation of the effects of power modulation on CTR is similar to that of pulse inversion as the same power series expansion can be performed. However, it is more complicated as the CTR is dependent on the amplitude level of the excitation. As power modulation uses two amplitude levels, there is not a single CTR to compare to. In general, however, the obtained CTR after processing will be equal or higher than the CTR in the high amplitude echo. As contrast agent is more non-linear than tissue, the CTR for the low amplitude excitation will be lower or equal to the CTR for the high amplitude excitation. Additionally, the absolute harmonic level for both tissue and contrast agent at low amplitude excitation cannot exceed their harmonic levels at high amplitude, even after the inverse scaling step of power modulation.

Lemma 1 *To prove that the CTR for power modulation after processing is equal or larger than the CTR obtained from the high amplitude excitation, we first observe that increasing excitation pressures give rise to increasing levels of harmonics relative to the fundamental. Therefore, after the inverse amplitude scaling step in power modulation we have*

$$C_H > C_L > 0$$
$$T_H > T_L > 0,$$

in which C_H and C_L are harmonic amplitude levels at high and low excitation pressures for

contrast agent and T_H and T_L are harmonic amplitude levels at high and low excitation pressures for tissue, respectively. Assuming that the high pressure echo has the higher CTR, we get

$$CTR_H = \frac{C_H}{T_H} \geq \frac{C_L}{T_L} = CTR_L.$$

Some rearranging gives

$$\begin{aligned} C_H T_L &\geq C_L T_H \\ C_H T_L - C_H T_H &\geq C_L T_H - C_H T_H \\ C_H(T_L - T_H) &\geq T_H(C_L - C_H) \\ \frac{C_H}{T_H} &\leq \frac{C_L - C_H}{T_L - T_H}, \end{aligned}$$

where we used in the last step the fact that $T_L - T_H$ is negative. Finally this gives

$$CTR_H = \frac{C_H}{T_H} \leq \frac{C_H - C_L}{T_H - T_L} = CTR_{PM},$$

in which the right term is exactly the CTR after the processing step of power modulation.

This implies, as is shown in Lemma 1, that the CTR for power modulation is equal or higher than the CTR in the high amplitude echo. As power modulation has a subtractive step, signal energy is lost. Therefore, the SNR will decrease. However, the decrease due this effect will be limited as the absolute level of the low amplitude harmonics is much lower as the absolute level of the high amplitude harmonics. In addition, the noise level will go up which further decreases the SNR by approximately 4.7 dB.

DESTRUCTION BASED DETECTION

Another approach to detection of contrast agent is based on destruction of the agent. When a contrast agent bubble is insonified at high ultrasound pressures (MI>0.1) it is generally destroyed by releasing its gas content into the blood. The destruction process produces a very distinct echo signal which can be used to detect the contrast agent. Additionally, the newly formed unencapsulated bubble has a different signature when interrogated with subsequent ultrasound pulses which can be used to detect the presence of contrast agent. Destruction based imaging operates by sending high amplitude destruction pulses in between the regular interrogation excitations at large time intervals. The destruction pulse destroys the contrast agent and leaves an area with short lived free gas bubbles. The change from encapsulated to unencapsulated contrast bubble can then be detected by correlating the received signal before and after the destruction pulse. However, as the contrast agent is destroyed in the process of detecting it and the unencapsulated bubbles are short lived, new agent has to flow into the imaging region through the blood flow after each destruction pulse which prevents a high imaging frequency.

Evaluation of this detection method on SNR and CTR differences is more difficult than for the previously described detection methods as the properties of the contrast agent change during the transition from encapsulated to unencapsulated bubble. In particular, the properties of the newly formed unencapsulated bubble are not well known as the destruction cannot be well controlled. Generally, however, a free gas bubble will scatter the ultrasound better than its encapsulated ancestor. Therefore, the signal energy in the received signal originating from the contrast agent will increase after the destruction pulse. Moreover, the correlational approach is very sensitive which further improves the SNR and CTR.

1.3 AIM OF THIS THESIS

Ultrasound contrast agent has been around for some time now in both experimental and clinical settings. From its initial discovery, a large amount of research has been focussed on the development of new and better contrast agents. This research has been complemented with the development of methods to detect the presence of the agent in tissue of which a few were described above. Although some of these detection methods perform well and are built into commercially available ultrasound equipment, they are generally not using much knowledge of the contrast agent bubble. Apart from the high scattering strength and high nonlinearity of the bubble, no other properties are used, in current methods, to obtain a high contrast to tissue ratio. In this area, therefore, improvements in the detectability of contrast agent and, hence, the contrast to tissue ratio are to be found by incorporating specific knowledge of a contrast agent bubble into the detection method.

This thesis explores three detection methods that do take into account the special properties of a contrast agent bubble. The first method is specifically aimed at the resonant nature of a bubble. Bubbles that are insonified around their resonance frequency react relatively slowly to the incident ultrasound pulse. Therefore, the large bandwidth ultrasound pulses currently in use for imaging do not excite the bubbles very well as their short time duration is too short to excite the bubble into a large radial oscillation. By using longer pulses and coded excitations, we aim to improve the response of the contrast agent without loss of axial resolution. We start exploring this method with a theoretical description of the method and a simulation study. Subsequently, we describe in-vitro experiments on a bubble suspension to confirm the results of the simulation study. Following this, the method is evaluated in an in-vitro phantom study to test its usability in an imaging situation. Finally, a bubble destruction experiment is described to quantify the limits of the detection method.

The second method is based on inducing and detecting changes in the physical properties of a contrast agent bubble. It is well known that the size of a bubble is an important factor in the response of a bubble to ultrasound insonification. This property is exploited by this method by using a low frequency conditioning signal to induce a change in the size of a bubble, and, simultaneously, detecting the change in

bubble response with a high frequency interrogation signal. We describe a method to detect the change in response, followed by simulation results. Finally, we show high speed camera observations that confirm the change in response on which this method is based.

The last method is based on the interaction between the non-linearity of a contrast agent bubble and the property of it being stateful in a system theoretic sense[37]. By using a special excitation sequence and subsequent processing it is possible to separate the confounded responses from tissue and contrast agent. This chapter shows a proof of concept and shows the direction in which the largest improvements in detection methods are to be sought. It describes the theoretical basis of the technique and a successful attempt to verify the theory with simulations and in-vitro measurements.

2 NON-LINEAR CODED EXCITATION METHOD FOR ULTRASOUND CONTRAST IMAGING

ABSTRACT

Coded excitation with compression on receive is used in medical ultrasound imaging to increase signal-to-noise ratio (SNR) and penetration depth. We performed a computer simulation study to investigate if chirped pulse excitation can be applied in ultrasound contrast agent imaging to increase SNR and contrast-to-tissue ratio and thus reduce contrast agent destruction and tissue harmonics. A new non-linear compression technique is proposed that selectively compresses the second harmonic component of the response. We compared a chirp of 9.4 μs duration, 2 MHz centre frequency, 45% relative bandwidth to a Gaussian pulse with equal centre frequency and bandwidth. For peak pressures between 50 and 300 kPa we found for resonant bubbles an increase in response between 10 and 13 dB. Moreover, the axial resolution after compression is comparable to axial resolution of conventional imaging. This effect is relatively insensitive to peak excitation pressure and is largest for bubbles having resonance frequency around the centre frequency of the excitation.

This chapter is based on the publication: J.M.G. Borsboom, C.T. Chin, and N. de Jong. Nonlinear coded excitation method for ultrasound contrast imaging. *Ultrasound Med. Biol.*, 29:277–284, 2003.

2.1 INTRODUCTION

In recent years, increasing interest has been shown in ultrasound contrast agent for both research and clinical use. Ultrasound contrast agent consists of small (1–10 μm diameter) gas-filled encapsulated microspheres that are small enough to pass lung circulation, enabling opacification of the left ventricle. Diagnostic ultrasound increasingly employs contrast agents for enhancement of ultrasound images. Strong linear scattering from contrast agent bubbles improves the response from hypo-echoic regions like blood, improving, for example, the delineation of the cavities and vessel structure of the human heart. Contrast agent in small blood vessels, however, is difficult to detect

from linear scattering due to the overlap in time and frequency domain of the echo from tissue and contrast agent.

Contrast agent bubbles are strong ultrasound scatterers that respond increasingly non-linearly when driven at increasing ultrasound pressures. High ultrasound pressures, however, break the shell and destroy the contrast agent. Research has been focusing on non-linear properties of contrast agent. Strong non-linear response from contrast agent enables discriminatory detection of contrast agent in tissue. Detection of contrast agent in tissue is useful for assessment of myocardial perfusion, an important goal in contrast agent research. Several techniques, mainly based on signal processing, have been proposed that detect the non-linear part of the scattered response; for example harmonic imaging[9, 38], pulse inversion[25] and power modulation[7]. These techniques process one or more traces from regular pulsed imaging sequences to detect the signal from the contrast agent while suppressing the signal from tissue. The performance of these methods is dependent on the relative levels of non-linearity from the contrast agent and the surrounding tissue due to non-linear propagation. The relative levels of non-linearity from contrast agent and tissue can be summarised in the contrast-to-tissue ratio. Optimisation of detection methods can be done either by developing a method with increased sensitivity for contrast agent or by changing the relative levels of non-linearity.

Regular pulse-echo imaging uses short, relatively high-powered pulses as they provide good axial resolution and high signal-to-noise ratio (SNR). Maximum peak pressure and pulse energy, however, are limited by regulatory agencies due to safety concerns. In 2-D greyscale imaging, for example, the peak transmitted pressure is mainly limited by the maximum mechanical index to avoid cavitation and tissue damage, while in colour Doppler the limit is usually the spatial peak, time average (SPTA). When using contrast agent, the peak transmitted pressure is not only limited by safety limits, but also by the destruction of the contrast agent and generation of tissue harmonics. As the latter limits usually are the tighter limits, the pulses used in contrast agent imaging contain less power and hence contrast agent imaging often has lower SNR than greyscale imaging. To increase the SNR one can either lower the noise level or increase the signal level. With coded excitation waveforms one can transmit more energy by using longer pulse durations without increasing peak pressures and decreasing pulse bandwidth. With proper decoding, axial resolution for coded excitation can be close to the axial resolution for a conventional pulse with equal bandwidth[30, 41].

Bubble dynamics can be approximately described as a damped mass-spring system. When driven by a constant amplitude sinusoidal excitation, the response of such a system can be divided into a transient and a steady state part. In the transient part the oscillation gradually builds up to constant amplitude, which indicates steady state. When bubbles are driven by conventional imaging pulses, the oscillation is in the transient regime due to the limited length of the pulse. Maximal oscillation amplitude is in most cases reached in steady state and therefore dependent on pulse length.

We propose a new contrast agent detection method based on coded excitation.

Coded excitation in medical ultrasound is used to increase SNR[36]. Higher SNR can be traded off to gain a greater penetration depth or improve visualisation of hypo-echoic regions. Properly designed codecs (coding-decoding) operate by transmission of a long pulse with relatively low peak amplitude, which is compressed at reception with a filter into a short pulse to obtain the necessary axial resolution and improved SNR. Improvements of more than 10 dB in SNR compared to regular pulsed imaging are reported[33]. However, range side lobes are introduced in the compressed signal. These side lobes can be reduced by proper apodisation of the transmitted pulse[42, 43].

In this paper we describe a simulation study investigating the potential of chirped excitation for contrast agent imaging. Apart from the increase in SNR from using chirped excitation, we expect that using a chirp pulse enhances non-linear scattering from a bubble. The longer time duration of the chirp may be able to excite the bubble closer into the steady state regime and maximise the oscillation amplitude of the bubble, giving larger response and more harmonics generation. Since propagation harmonics are dependent on peak amplitude and not pulse energy[26], it may be possible to lower the level of tissue harmonics relative to the contrast harmonics. By extracting the second harmonic from the received signal with a new chirp compression method aimed at the non-linear part of the response, we can discriminate between tissue and contrast agent.

2.2 THEORY

Bubble dynamics of a contrast agent bubble suspended in a liquid can be approximately described as a damped non-linear mass-spring system. The following modified Rayleigh, Plesset, Noltingk, Neppiras and Poritsky (RPNNP) differential equation describes bubble radius as a function of time when insonified with ultrasound[15]. In this equation the shell stiffness and the shell friction parameterise the bubble.

$$\rho R\ddot{R} + \frac{3}{2}\rho\dot{R}^2 = p_{go}(\frac{R_0}{R})^{3\Gamma} + p_v - p_{lo} \\ -\frac{2\sigma}{R} - 2S_p(\frac{1}{R_0} - \frac{1}{R}) - \delta_t\omega\rho R\dot{R} - p_{ac}(t), \qquad (2.1)$$

where

R = instantaneous bubble radius
ρ = density of surrounding medium
R_0 = initial bubble radius
P_{go} = initial gas pressure inside the bubble
Γ = polytropic exponent of the gas
p_v = vapour pressure
p_{lo} = hydrostatic pressure

σ = surface tension coefficient
δ_t = total damping coefficient
ω = angular frequency of incident acoustic field
$p_{ac}(t)$ = time varying pressure of incident acoustic field
S_p = shell stiffness parameter.

The initial gas pressure and the total damping coefficient are given by

$$\begin{aligned} p_{go} &= \frac{2\sigma}{R_0} + p_{lo} + p_v \\ \delta_t &= \delta_{rad} + \delta_{vis} + \delta_{th} + \delta_f \\ \delta_f &= \frac{S_f}{m\omega}, \end{aligned}$$

where

δ_{rad} = damping coefficient due to re-radiation
δ_{vis} = damping coefficient due to viscosity of surrounding liquid
δ_{th} = damping coefficient due to heat conduction
δ_f = damping coefficient due to friction inside the shell
S_f = shell friction parameter
m = effective mass of bubble-liquid system.

Expressions for the damping coefficients and the effective mass are given by Medwin[28].

A computer program was developed in Matlab (The Mathworks, Inc., Natick, MA, USA) and C to solve this equation for a predefined excitation. The differential equation was solved using a fifth order Runge-Kutta algorithm with variable step size[35]. With this tool the effects of different excitation signals on the scattering efficiency of contrast agent bubbles were investigated. Scattering efficiency is quantified by the scattering cross-section, which is defined as the ratio of scattered power and incident intensity.

We expect that longer pulses will generate larger oscillation amplitudes of the bubble wall and thus increase the generation of harmonics. Longer pulses, however, generally compromise axial resolution. Improved pulsing for contrast agent imaging is possible if a long pulse with good axial resolution can be used. Coded excitation combines longer pulses with good axial resolutions. Coded excitation operates by transmitting a relatively long pulse with low peak amplitude but maintains bandwidth for good axial resolution. By using long pulse lengths more energy is transferred into the medium compared to a single Gaussian pulse with equal bandwidth and peak amplitude. After processing the received signal good axial resolution and high SNR can be obtained.

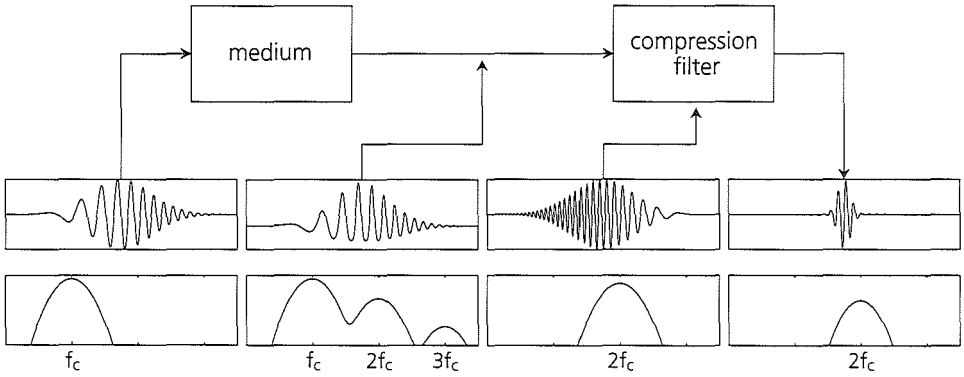

Figure 2.1: Overview of compression method for selective compression of second harmonic part in bubble response.

A special type of coded excitation signals is called chirp. Chirps are long bursts with increasing or decreasing instantaneous frequency. After reception, the received echo signal needs to be processed to recover axial resolution. Processing of this signal, called compression, is performed by filtering this signal with a specific compression filter. After compression, the resulting signal has better axial resolution than the initially received signal. However, in the compression process, range side lobes are introduced. Proper codec design suppresses these side lobes to acceptable levels. A class of chirps well suited for ultrasound purposes are the so-called quadratic chirps. In these chirps the instantaneous frequency changes linearly with time. An important property of these chirps is the robustness against frequency shifts due to attenuation[30]. The main design parameters of these chirps are the time-bandwidth product and the apodisation window. The compression filter in general has an impulse response equal to the time inverse of the chirp used as excitation.

Conventional compression operates on the same bandwidth as the excitation chirp and the harmonics are suppressed. In order to extract higher harmonics from the received bubble signal, we propose a new type of compression filter. Figure 2.1 shows a schematic of this new compression technique. Instead of using the same chirp for excitation and compression, which is used in the matched filtering approach, the compression chirp has double frequency at every point compared to the excitation chirp. In frequency domain this means that the bandwidth of the compression filter coincides with the second harmonic generated by the bubble. By filtering the response through this compression filer, we extract the second harmonic from the bubble response and adjust phases to obtain good axial resolution. For example, when the excitation chirp ranges from 2 MHz to 4 MHz, the compression filter will have as impulse response a chirp ranging from 8 MHz to 4 MHz.

To investigate the effect of pulsed excitation, which has large bandwidth and short

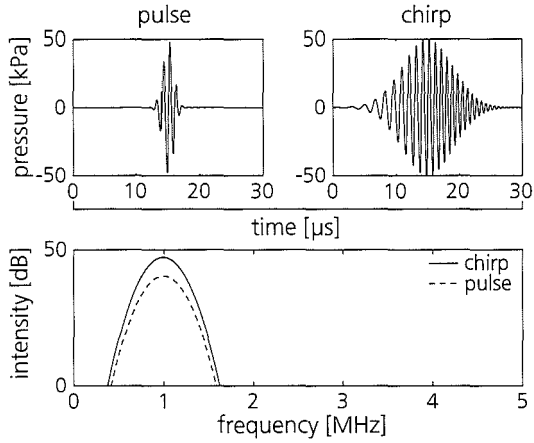

Figure 2.2: Gaussian pulse and quadratic chirp apodised with Gaussian window that have equally shaped Fourier magnitude spectra.

time duration, and chirped excitation, which has large bandwidth and long time duration, on a contrast agent bubble, we designed Gaussian pulses and quadratic chirps with approximately the same magnitude spectrum, but differing in their phase spectra. Figure 2.2 shows a two cycle (45% relative bandwidth) Gaussian pulse and a quadratic chirp apodised with a Gaussian window, in both time and frequency domain. It is shown that while the two signals have the same magnitude spectrum, they have very different lengths in time domain. The –6 dB length of the pulse is approximately 2.0 μs, while for the chirp it is 9.4 μs. Using these signals as excitation for a linear system would not give much difference in the magnitude spectra of the output signals, as the equal magnitude spectra in the input signal are conserved in the output signal of the linear system. Non-linear systems, on the other hand, may show different spectral responses from input signals with equal magnitude spectra but differing phase spectra. The pulse and the chirp were used as excitation in a bubble response simulation. Simulation parameters for the bubble were set for a SonoVue™ bubble suspended in water[21].

Contrast agent suspension contains bubbles with varying sizes and resonance frequencies. To check the efficiency of chirps for bubbles of various sizes, single bubble simulations were performed using pulse and chirp as excitation for SonoVue bubbles ranging in radius from 1 μm to 4 μm. Simulated responses were filtered to extract the second harmonic part of the response for pulsed excitation and compressed with the harmonic compression filter for chirped excitation.

Table 2.1: Peak reflected pressure (Pa) at 1 cm from a 3 μm free gas bubble excited at 50 kPa peak pressure for several bandwidths.

	11% bandwidth	45% bandwidth	100% bandwidth
pulse	322	90	45
chirp	330	232	174

2.3 RESULTS

Conventional pulsed imaging systems use broadband pulses to obtain high axial resolution. The short duration of these pulses prevent a contrast agent bubble to reach maximal oscillation amplitude. Longer pulse durations produce larger oscillation amplitudes and therefore enhance contrast agent detectability. Figure 2.3(a) shows the scattered pressure at 1 cm from a 3 μm radius free gas bubble with resonance frequency 1 MHz excited by Gaussian envelope pulses of eight (11% relative bandwidth), two (45%) and 0.9 (100%) cycles with peak amplitude 50 kPa and centre frequency 1 MHz. The figure shows that for excitation pulses with equal peak pressures and different pulse lengths, the amplitude of the reflected pressure is approximately six times higher for an eigth cycle pulse than for a 0.9 cycle pulse. Figure 2.3(b) shows the scattered pressure at 1 cm for the same free gas bubble, but excited with chirps with equal centre frequencies, bandwidths and peak amplitudes as for Fig. 2.3(a). The length of the chirps is 9.4 μs. The amplitude of the reflected pressure is almost four times higher for wideband chirp compared to an equal bandwidth pulse. Table 2.1 summarises Figs. 2.3(a) and 2.3(b). The table shows the peak pressures at 1 cm from the bubble for both excitation waveforms for the three relative bandwidths. Compared to equal bandwidth Gaussian pulses, the chirp generates a larger response from the bubble, in particular when the bandwidth is large. This effect is strongest for bubbles insonified at their resonant frequency. For tissue the amplitude response is directly dependent on the excitation amplitude. Pulse length, therefore, has no effect on scattered pressure for tissue.

Figure 2.4 shows the responses shown in Figs. 2.3(a) and 2.3(b) in frequency domain. Each subfigure shows the response of a free gas bubble to a pulse and a chirp of equal bandwidth and peak amplitude. In all figures the level of the fundamental for pulsed excitation is lower than the fundamental for chirped excitation which is due to the energy difference in the excitation pulses. The differences between the fundamentals from pulsed and chirped excitation that are expected from the energy differences in the excitations, are 1.4 db, 6.8 dB and 10.3 dB. These values agree well with the values found in Fig. 2.3. The difference between the second harmonics is equal or larger than the difference between the fundamentals. Observed differences are –0.1 dB, 8.7 dB, and 15.1 dB. Taking the response from pulsed excitation as baseline, this in-

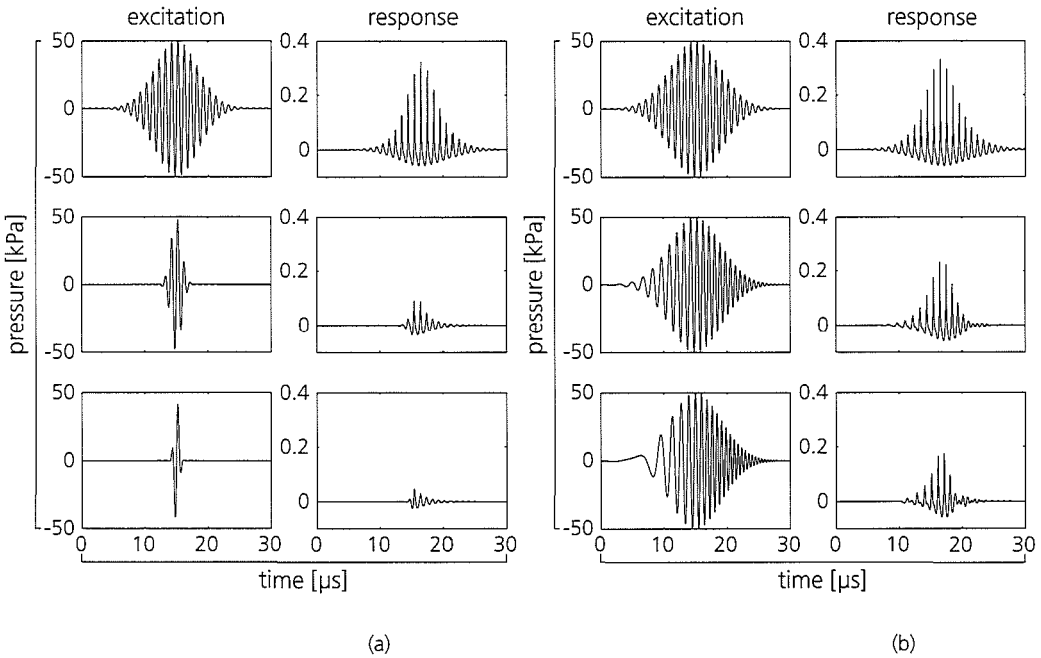

Figure 2.3: Pressure response at 1 cm from a 3 μm radius free gas bubble, excited with (a) 8, 2 and 0.9 cycle Gaussian pulses with peak amplitude 50 kPa and centre frequency 1 MHz, and with (b) chirps with peak amplitude 50 kPa and relative bandwidths of 11%, 45% and 100% that equal the bandwidths and centre frequencies of the Gaussian pulses in (a).

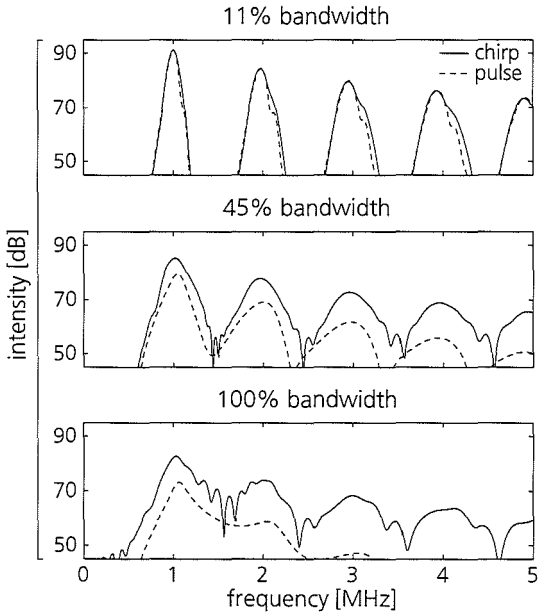

Figure 2.4: Response in frequency domain at 1 cm for a 3 μm radius free gas bubble, excited with pulses and chirps with peak amplitude 50 kpa and 11%, 45% and 100% bandwidths.

dicates improved response from chirped excitation when the duration of the chirp is longer than the equal bandwidth pulse. This shows that not only the bandwidth but also the duration of the excitation is a determinant for harmonics generation.

Figure 2.5 shows the simulated pressure response at 1 cm from the surface of a 2.75 μm radius contrast agent bubble in time and frequency domain excited with the pulse and chirp as defined in Fig. 2.2 with 150 kPa peak pressure. It is clear that the pressure response for the chirp has higher peak amplitude than the response for the pulse. The difference in frequency domain between the fundamentals is approximately 10 dB, which is mainly the energy difference in the excitation signal. For the second harmonic, the difference between the peaks is 13 dB, indicating an improved response above that which can be expected from the difference in input energy.

Increased harmonics generation for chirped excitation is relatively independent of peak pressure. Figure 2.6 shows the peak level of fundamental and second harmonic of the simulated response as a function of insonified peak pressure. Excitations were pulse and chirp with peak pressures of 50, 150 and 300 kPa. It is clear that the absolute level of the response increases for increasing excitation pressure. The improved response of chirped excitation compared to pulsed excitation for the second harmonic is

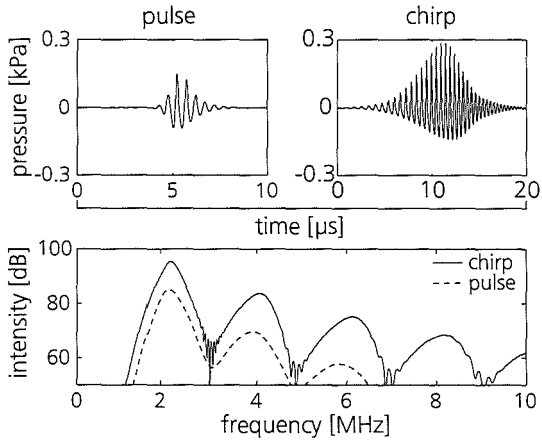

Figure 2.5: Simulated pressure at 1 cm from a 2.75 μm radius contrast agent bubble, when excited with a two cycle Gaussian pulse and equal bandwidth chirp, both with peak amplitude 150 kpa and centre frequency 2 MHz.

present for all excitation pressures. With chirped excitation, therefore, lower excitation pressures can be used, without sacrificing SNR and harmonics level.

Compression of the simulated echo from a contrast agent bubble was performed with a conventional compression filter and the newly defined second harmonic compression filter, which filter out and compress the fundamental and the second harmonic in the response. Both the conventional and the harmonic compression filter had the same bandwidth as the excitation chirp, differing only in the centre frequency of the filter response. Figure 2.7 shows on logarithmic scale the envelope of the compressed fundamental and second harmonic response of a 2.75 μm SonoVue bubble excited with a 150 kPa peak pressure chirp. After compression, the responses show an axial resolution of 2.68 mm for the fundamental and 1.95 mm for the second harmonic. Side lobes are present at more than −50 dB though not visible and −37 dB below the main lobe. Table 2.2 shows axial resolutions for both fundamental and second harmonic when using pulses and chirps with various relative bandwidths as excitation. Axial resolution for a 45% bandwidth chirp is within 15% of the axial resolution obtained from equal bandwidth pulsed excitation, indicating relatively good compression performance. Axial resolution for a 100% bandwidth chirp is worse than expected due to the high side-lobe level after compression. Table 2.3 shows side-lobe levels after harmonic compression for chirps with various relative bandwidths. Increasing the bandwidth of the excitation increases the side lobe level after compression, indicating a trade-off between bandwidth and side lobe level.

Contrast agent suspension contains bubbles with varying sizes and resonance fre-

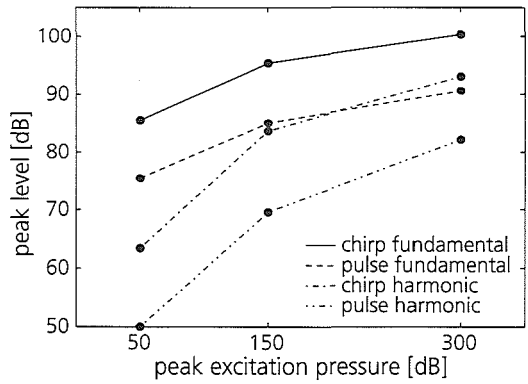

Figure 2.6: Peak level of fundamental and second harmonic at 1 cm from a 2.75 μm radius contrast agent bubble for chirp and pulse excitation with peak pressures of 50, 150 and 300 kPa.

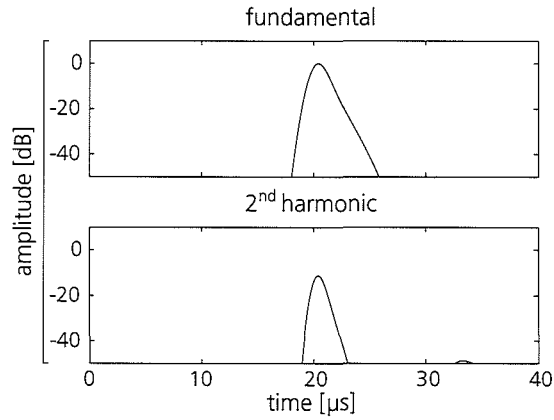

Figure 2.7: Compressed fundamental and second harmonic response for a 2.75 μm radius contrast agent bubble excited with a 45% bandwidth chirp at 150 kPa.

Table 2.2: Axial resolution (mm) for fundamental and second harmonic for a 2.75 μm contrast agent bubble for several bandwidth excitations

	11% bandwidth		45% bandwidth		100% bandwidth	
	fundamental	2nd harm.	fundamental	2nd harm.	fundamental	2nd harm.
pulse	11.09	7.69	2.64	1.71	1.61	0.70
chirp	13.60	9.76	2.68	1.95	1.67	1.27

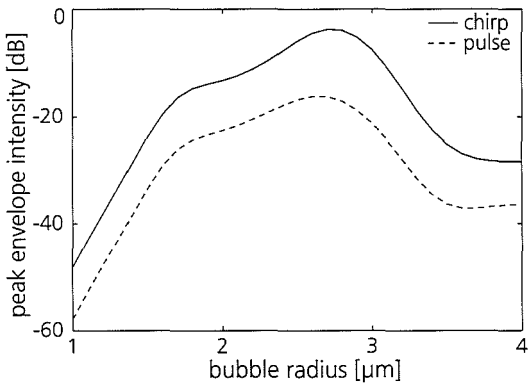

Figure 2.8: Peak second harmonic envelope intensity for contrast agent bubbles with different radii, excited with 45% bandwidth, 150 kPa peak pressure Gaussian pulse and Gaussian apodised chirp.

quencies. To check the efficiency of chirps for bubbles of various sizes, single bubble simulations were performed using the pulse and chirp from Fig. 2.2 at 150 kPa as excitation for SonoVue bubbles ranging in radius from 1 to 4 μm. Simulated responses were filtered to extract the second harmonic part of the response for pulsed excitation and compressed with the harmonic compression filter for chirped excitation. Figure 2.8 shows the peak second harmonic envelope and harmonic compressed envelope of both excitations. The effect of the chirp giving higher response for every bubble size is easily appreciated. In addition, it can be seen that this effect is strongest when the resonance frequency of the bubble is near the centre frequency of the excitation. In this case this corresponds to a bubble with 2.75 μm radius having resonance frequency 2 MHz.

Table 2.3: Side-lobe level (dB) after harmonic compression for a 2.75 μm contrast agent bubble for several bandwidth excitations

	11% bandwidth	45% bandwidth	100% bandwidth
side-lobe level (dB)	−100	−37	−3.5

2.4 DISCUSSION

Looking at the response from a free gas bubble for a Gaussian pulse with different numbers of cycles as excitation in Fig. 2.3(a), it is shown that if we excite a bubble with a longer pulse while keeping peak amplitude constant, the bubble generates a larger response. For the fundamental this is what we expect from linear system theory, as a pulse with more cycles contains more energy around the centre frequency of the pulse. The energy in the harmonics that are generated by the non-linear bubble system, increase as well, both absolutely and relatively to the energy in the fundamental. This means that for fixed amplitude for the excitation pulse, the longer pulse generates more harmonics. As tissue harmonics generation is mainly dependent on the peak amplitude of the excitation pressure pulse, the contrast to tissue ratio increases when using longer pulses.

Chirped excitation signals use longer pulse length to increase pulse energy without increasing peak amplitude. With compression increased SNR and good axial resolution can be obtained. Using the 9.4 μs, 45% relative bandwidth chirp as defined earlier, we expect a theoretical increase in SNR of approximately 10 dB. The level of the second harmonic was shown in Fig. 2.6 to increase by approximately 13 dB relatively independent of peak pressure in the excitation pulse. By selective compression of the second harmonics, we can obtain axial resolutions comparable to axial resolutions from equal bandwidth Gaussian pulses as is shown in table 2.2. For 100% bandwidth chirps, axial resolution for harmonic compression decreases sharply due to elevated side-lobe levels. Good codec design is necessary to suppress the range side-lobes when using more broadband chirps. Table 2.3 showed that side-lobe levels after harmonic compression increase for chirps with increasing relative bandwidths. The high side-lobe level of the broadband chirp prohibits the use of chirps with very large frequency ranges. Overlap in fundamental and second harmonic appears after compression as elevated side-lobe levels. For contrast imaging a side-lobe level of −20 dB is acceptable. The overlap can be suppressed by using pulse inversion like techniques. This is currently under investigation.

A suspension of bubbles of varying sizes as present in real contrast agent produces a larger response when excited by a chirped excitation signal. The largest response from a single bubble is obtained when the resonance frequency of the bubble is near the centre frequency of the chirp. By matching frequency range of the chirp to the

size distribution of the contrast agent, an optimal response from real contrast agent suspension is expected.

We have developed a new method for contrast agent imaging that uses a chirp instead of a pulse as excitation. By selectively compressing the second harmonic part of the response, improved signal to noise ratio and contrast to tissue ratio can be obtained. Using a well designed codec we can obtain good axial resolution and low side-lobe levels. Combination of chirped excitation with known methods like pulse inversion is currently under investigation.

3 EXPERIMENTAL EVALUATION OF A NON-LINEAR CODED EXCITATION METHOD

ABSTRACT

Previously, we have shown that for a single bubble, using chirps as the excitation signal improves both the linear and the non-linear response. Computer simulations of randomly distributed contrast agent bubbles show an increase of 10–13 dB in response when comparing pulse excitations with chirp excitations that have equal bandwidths and peak amplitudes. Second harmonic compression of simulated bubble echoes with chirp excitation shows low side-lobe levels and limited loss of axial resolution when compared to pulse excitation. Experimental results from water tank measurements with SonoVue™ contrast agent are in agreement with computer simulations showing increased signal-to-noise ratio and an increase of approximately 12 dB at the second harmonic when comparing pulse and chirp excitation.

This chapter is based on the publication: J.M.G. Borsboom, C.T. Chin, and N. de Jong. Experimental evaluation of a non-linear coded excitation method for contrast imaging. *Ultrasonics*, 42:671-675, 2004.

3.1 INTRODUCTION

Ultrasound contrast agent imaging with low mechanical index (MI) is increasingly employed in clinical settings and object of increasing research interest[1]. Ultrasound contrast agent consists of small (1–10 μm diameter) gas-filled encapsulated micro-spheres that are small enough to pass lung circulation, enabling opacification of the left ventricle. Like unencapsulated air bubbles, contrast agent bubbles are strong ultrasound scatterers, both linearly and non-linearly[27]. Linear scattering from contrast agent bubbles improves the response of hypo-echoic regions like blood, improving for example the delineation of the cavities of the human heart. Non-linear scattering enables discriminatory detection of contrast agent in tissue. Special methods have been developed to detect non-linear scattering in the received signal, for example harmonic imaging, pulse inversion and power modulation[38, 25, 7]. However, both tissue and

contrast agent scatter non-linearly, confounding their relative contributions to the received signal.

Conventional imaging uses short, relatively high-powered pulses as they provide high axial resolution and good signal-to-noise ratio (SNR). Peak transmitted pressure and pulse energy, however, are limited by regulatory agencies due to safety concerns. In 2-D greyscale imaging, for example, the peak transmitted pressure is mainly limited by the maximum MI to avoid cavitation and hence tissue damage, while in colour Doppler the limit usually is the spatial peak temporal average intensity (ISPTA). When using contrast agent, the peak transmitted pressure is also limited by the destruction of the contrast agent. As the latter limit is usually the lower one, the pulses used in non-destructive contrast agent imaging exhibit a low power. Therefore, contrast agent imaging usually produces a lower SNR than greyscale imaging. To increase the SNR one can either lower the noise level or increase the signal level. With special coding techniques one can increase pulse energy by transmitting longer pulses without increasing peak pressure and without decreasing pulse bandwidth. With proper decoding, axial resolution is not compromised[31].

Our research focuses on a type of coded excitation signal called chirp for use with contrast agent imaging. Chirps are long, possibly amplitude apodised, bursts with increasing or decreasing instantaneous frequency. We use so-called quadratic chirps in which the instantaneous frequency increases linearly with time. Conventionally, chirps are used in ultrasound imaging to increase SNR when peak transmitted pressure is limited. Improvements of more than 10 dB in SNR have been reported[33]. Imaging with chirped excitation signals operates by transmission of the chirp into the medium. The subsequently received echo is processed to obtain an image with axial resolution that is comparable to axial resolution from regular pulse excitation. The process in which the received echo regains the axial resolution that is to be expected from the bandwidth of the transmitted excitation signal is called compression and is usually performed by passing the signal through a compression filter. However, in this process, range side lobes are introduced in the compressed response. These side lobes can be reduced by proper apodisation of the transmitted chirp[42]. Conventional compression filters operate on the same bandwidth as the excitation signal, hence suppressing the harmonics in the response. We have proposed a new type of compression filter that performs compression on the harmonic part of the response[3]. By filtering the received echo through this compression filter, we extract the second harmonic and adjust phases to obtain good axial resolution.

In this paper we describe a simulation study of the advantages of chirped excitation for contrast agent imaging and the subsequent experimental validation. First, simulation results for clouds of bubbles with realistic size distributions are shown. Subsequently, we show the performance of the compression filters on simulated echoes from single bubbles. Finally, we present water tank measurements to validate the results from the simulation study.

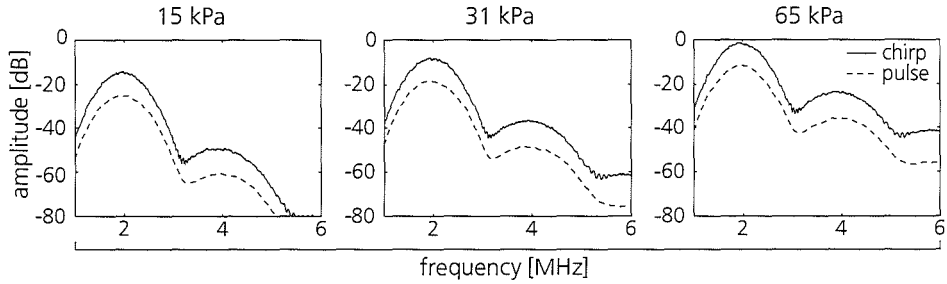

Figure 3.1: Simulated frequency domain response of a cloud of 7000 randomly distributed contrast agent bubbles excited with chirp (—) and pulse (---) with equal bandwidth and peak amplitude, using different peak pressures.

3.2 SIMULATIONS

Using a modified Rayleigh, Plesset, Noltingk, Neppiras and Poritsky (RPNNP) differential equation with parameters of SonoVue (Bracco Research SA, Geneva, Switzerland)[12, 21], which relates the time varying bubble radius to the applied excitation pressure, the response of a single contrast agent bubble was calculated. Using a size distribution for the bubble radii and shifting the individual bubbles responses randomly in time before summing the individual responses, we approximate the response from a bubble population. Figure 3.1 shows the average frequency domain pressure response of a cloud of 7000 bubbles with SonoVue size distribution and randomly distributed in space. As excitation we used 2 MHz, 45% fractional bandwidth Gaussian pulses and equal centre frequency and bandwidth Gaussian apodised quadratic chirps with peak pressures of 15 kPa, 31 kPa, and 65 kPa. At these pressures we see differences at the fundamental of 10.5 dB, 10.0 dB, and 9.8 dB between pulse and chirp excitation. This is in agreement with a difference of 10 dB in the excitation signals. The differences at the second harmonic are 10.9 dB, 11.9 dB, and 11.7 dB for the three excitation pressures, showing a slightly increased second harmonic relative to the fundamental for higher excitation pressures. This is as expected from previous single bubble simulations[3].

Compression performance of the harmonic compression technique was evaluated using simulated single bubble echoes. Simulated bubble echoes from chirp excitation were compressed using both a conventional compression filter and a second harmonic compression filter and compared to the responses from equal bandwidth and centre frequency pulses. Figure 3.2 shows, on logarithmic scale, the envelope of the compressed fundamental and second harmonic response for a 2.75 μm contrast agent bubble and the envelope of the filtered fundamental and second harmonic response for the same bubble. Excitations were as defined for Fig. 3.1 at peak pressure 150 kPa. After compression, the responses show an axial resolution of 2.8 mm for the fundamental and

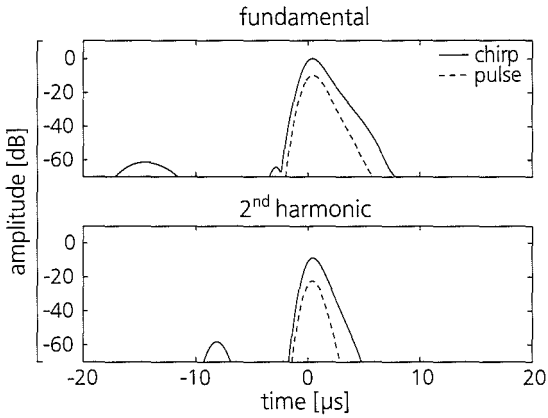

Figure 3.2: Envelope of fundamental and second harmonic response for a simulated 2.75 μm radius contrast agent bubble excited with chirp (—) and pulse (---) with equal bandwidth and peak amplitude.

2.3 mm for the second harmonic. This compares well to the axial resolutions of pulse excitations, i.e. 2.7 mm for the fundamental and 2.0 mm for the second harmonic. Side-lobes are present at –60 dB and –50 dB below the main lobe.

3.3 MEASUREMENTS

For validation of the simulation results we performed water tank measurements on SonoVue contrast agent. A small, acoustically transparent container was filled with a 1:10,000 dilution of SonoVue and placed in a water tank at the confocal point of two perpendicularly mounted broadband transducers as shown in Fig. 3.3. One transducer (PZT, Ø 32 mm, 75 mm focal length, 2.25 MHz centre frequency (Panametrics, Waltham, MA, USA)) was used for transmission, the other (composite, Ø 15 mm, unfocussed, 3.5 MHz centre frequency (Imasonic SA, Besançon, France)) for reception. Excitations were generated by an arbitrary waveform generator (LW420A, LeCroy, Chestnut Ridge, NY, USA) and amplified by a 50 dB linear power amplifier (2100L, ENI, Rochester, USA). The amplitude was adjusted with a variable attenuator (355C/D, HP, Palo Alto, CA, USA). The transmission transducer was excited with either a 2 MHz centre frequency, 45% fractional bandwidth Gaussian envelope pulse with 0.75 μs duration or an equal bandwidth and equal centre frequency Gaussian apodised quadratic chirp with 9.6 μs duration. The excitations were calibrated with a PVDF needle hydrophone (Precision Acoustics Ltd., Dorchester, UK) in gas saturated water to have the same peak pressure at the focus of the transducer. Peak negative pressures ranged between 15 kPa and 150 kPa, which corresponds at 2 MHz with MI's

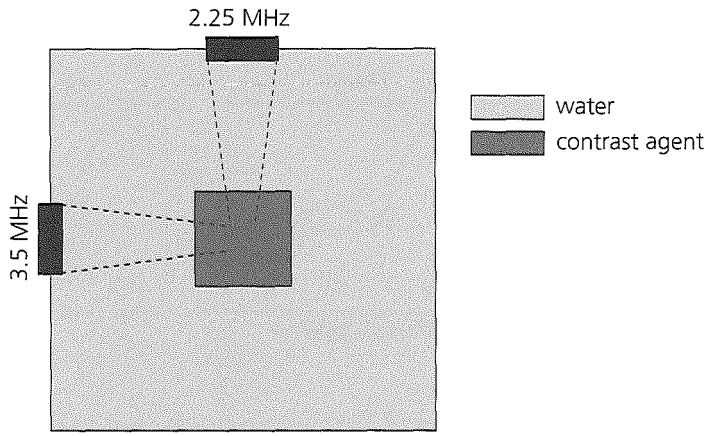

Figure 3.3: Schematic setup for contrast agent scattering measurements.

between 0.01 and 0.1[13]. The response of the contrast agent was received with the 3.5 MHz transducer, amplified, and digitised with an 8-bit digital oscilloscope (9400A, LeCroy, Chestnut Ridge, NY, USA) and recorded through an IEEE 488 interface on a personal computer.

Figure 3.4 shows frequency domain responses averaged over 250 traces for pulse and chirp excitation at peak excitation pressures of 15 kPa, 31 kPa, and 65 kPa. All curves are corrected for the bandwidth of the receiving transducer. The difference between the curves at the 2 MHz fundamental is 7.1 dB at 15 kPa excitation and 9.2 dB at 31 kPa and 65 kPa excitation. This is in agreement with an expected difference of 9.7 dB, which is the energy difference between pulse and chirp excitation. The error in the pulse-chirp difference at 15 kPa excitation is due to the low SNR in the measurement. At the 4 MHz second harmonic the difference between the curves is 12.3 dB at 15 kPa excitation, 5.6 dB at 31 kPa and 11.4 dB at 65 kPa.

Experimental validation of the harmonic compression technique was performed by compression of harmonics from non-linear propagation. Figure 3.5 shows, on logarithmic scale, the envelope of the compressed fundamental and second harmonic of an echo from a Perspex block, insonified at high pressure to improve harmonics generation. Excitations were again as defined for Fig. 3.1 at a peak pressure of approximately 1 MPa. It is shown that, except for an increase in energy, the curves for pulse and chirp excitation are very similar, indicating that axial resolution does not deteriorate much when comparing chirp to pulse excitation. This is true for both the fundamental and the second harmonic curves. Side-lobes are visible for the compressed chirp curves at −60 dB and −40 dB for fundamental and second harmonic respectively.

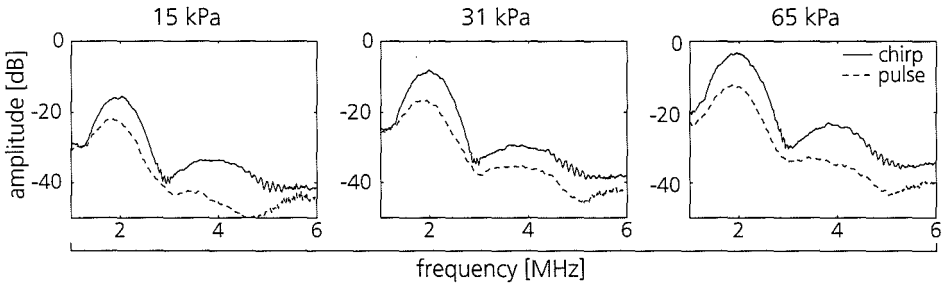

Figure 3.4: Frequency domain response of 250 measured traces from contrast agent for chirp (—) and pulse (---) with equal bandwidth and peak amplitude, using different peak pressures.

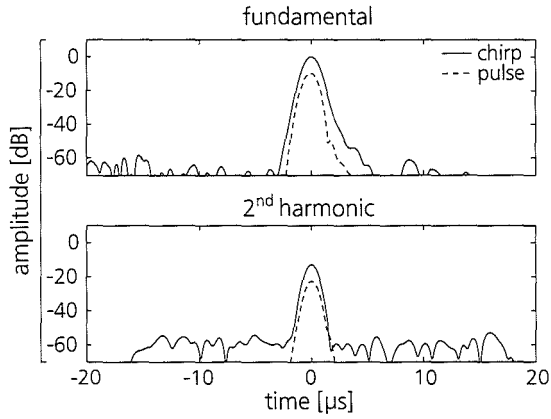

Figure 3.5: Envelope of fundamental and second harmonic response from non-linear propagation using chirp (—) and pulse (---) excitations with equal bandwidth and peak amplitude.

3.4 DISCUSSION

To avoid bubble destruction, contrast agent imaging is usually performed at low MI. However, at low MI the SNR is compromised. An increase in SNR can be obtained, though, by using longer, chirped excitation signals with compression on receive to regain axial resolution. Both the simulations in Fig. 3.1 and the measurements in Fig. 3.4 show an increase of approximately 10 dB in signal level when comparing pulse to chirp. Assuming approximately equal noise levels for both excitations, which is not unrealistic as the bandwidths of the excitations are equal, this amounts to an improvement in SNR of 10 dB. Previously reported single bubble simulations have shown an additional increase up to 3 dB for the second harmonic when insonifying a bubble around its resonance frequency. This increase is apparent in the simulation results of Fig. 3.1, though less pronounced. This is due to the inability to insonify all contrast agent bubbles in a size distribution at their resonance frequencies. The measurement results in Fig. 3.4 indicate some increase as well, but the increase is not consistent over the excitation pressures.

When using chirp excitation, the quality of the signal after compression can be defined in terms of main-lobe width (resolution) and side-lobe level. Using Fig. 3.2 and Fig. 3.5 we can compare compression performance of simulated bubble echoes and measured non-linear propagation echoes. Although the mechanism that generates the harmonics in non-linear propagation is different from the mechanism in bubbles, compression of the echo from non-linear propagation gives experimental insight in the feasibility and base-line performance of the compression technique. Evaluating the performance of the compression filter on non-linear propagation and bubble echoes, we see that the main-lobes for compressed chirp are all similar to the main-lobes for uncompressed pulse, indicating only a slight loss in axial resolution for chirp excitation. Side-lobe levels are below -60 dB for the fundamental and below -50 dB for the second harmonic for both simulated and measures echoes. As these levels are relatively low, this provides a possibility to trade off side-lobe levels for excitation bandwidth. Although increasing the bandwidth increases the side-lobes levels[3], side-lobes at -30 dB are still usable for contrast agent imaging, especially when the sensitivity to contrast agent is increased by the method. In addition, we can use pulse inversion to suppress neighbouring harmonics and hence side-lobes.

Using chirps as excitation signal for contrast agent imaging has been shown to improve SNR without decreasing axial resolution. Improved harmonic response has been seen in simulations, but the measurements are not yet conclusive. However, as we expect bubble destruction to be mostly dependent on peak pressure and to a lesser extent on pulse energy, chirp excitation may provide a method to decrease bubble destruction without a significant decrease in image quality. This trade off is currently under investigation.

4 HARMONIC CHIRP IMAGING METHOD FOR ULTRASOUND CONTRAST AGENT

ABSTRACT

Coded excitation is currently used in medical ultrasound to increase signal-to-noise ratio (SNR) and penetration depth. We propose a chirp excitation method for contrast agents using the second harmonic component of the response. This method is based on a compression filter that selectively compresses and extracts the second harmonic component from the received echo signal. Simulations have shown a clear increase in response for chirp excitation over pulse excitation with the same peak amplitude. This was confirmed by 2-D optical observations of bubble response with a fast framing camera. To evaluate the harmonic compression method we applied it to simulated bubble echoes, to measured propagation harmonics and to B-mode scans of a flow phantom and compared it to regular pulse excitation imaging. An increase of approximately 10 dB in SNR was found for chirp excitation. The compression method was found to perform well in terms of resolution. Axial resolution was in all cases within 10% of the axial resolution from pulse excitation. Range side-lobe levels were 30 dB below the main lobe for the simulated bubble echoes and measured propagation harmonics. However, side-lobes were visible in the B-mode contrast images.

This chapter is based on the manuscript: J.M.G. Borsboom, C.T. Chin, A. Bouakaz, M. Versluis, and N. de Jong. Harmonic chirp imaging method for ultrasound contrast agent. Accepted for publication in *IEEE Trans. Ultrason. Ferroelec. Freq. Contr.*

4.1 INTRODUCTION

In the last decade, several new pulsing schemes and signal processing methods were developed for ultrasound contrast imaging. Regular diagnostic imaging saw the advent of harmonic imaging and multi-pulse excitation schemes like pulse inversion and power modulation[38, 25, 7]. These methods, which rely on selective extraction of spectral components in the received echo, have shown to provide significant improvements in image quality and contrast-to-tissue ratio (CTR). More recently, coded excitation was introduced. Coded excitation operates by transmission of long pulses in which a

clearly recognisable signature, the 'code', is embedded[41]. After reception, the resulting echo signal is filtered through an autocorrelation-based filter to detect and remove the code; a process called decoding or compression. A good code is well detectable in the received echo and encompasses more bandwidth than an equal length Gaussian pulse. At compression time, this bandwidth is used to obtain good range resolution. As the axial resolution after decoding depends on the bandwidth of the excitation signal, images with good axial resolution can be obtained using long pulses combined with coded excitation. However, range side-lobes may result from decoding due to a partial match of the code and the compression filter for certain time shifts.

Codes suitable for ultrasound applications can be divided into two categories based on the type of coding[30]. One category consists of codes based on phase modulated signals. In these codes a long sinusoidal burst of constant frequency is modulated by alternating the phase of subsequent parts of the sinusoid over a fixed set of phase values. For example, for binary codes like Barker codes and Golay codes the phase alternates between 0° and 180°. The other category consists of codes based on frequency modulation. In these codes the instantaneous frequency of a long sinusoidal burst is modulated over time. For ultrasound imaging, the most important code in this category is the linear frequency sweep or linear chirp as it is relatively robust to frequency shifts. In general, a shift in mean frequency is found in signals received from frequency dependent attenuating media like tissue. This attenuation, which is approximately proportional to frequency, causes the chirp to be shifted downward in frequency. However, as the frequency shift translates after decoding into a time shift, the response from an attenuating medium will only be slightly shifted in time, which is acceptable for imaging purposes[30]. A linear chirp is a long sinusoidal burst with an instantaneous frequency changing linearly in time. The amplitude may be apodised to suppress range side-lobe generation from the decoding filter[42]. Conventionally, chirps have been used to increase the signal-to-noise ratio (SNR) when peak transmission amplitude is limited. SNR improvements of more than 10 dB have been reported[33].

Currently available ultrasound contrast agents consist of small (1-10 μm diameter) gas-filled encapsulated micro-spheres. Like free air bubbles, contrast agent bubbles are strong ultrasound scatterers, both linearly and non-linearly. Strong non-linear scattering from contrast agents enables discriminatory detection in tissues, which is employed in several nonlinear contrast agent imaging methods. The performance of these methods is dependent on the relative contributions of the non-linear response from contrast agent and surrounding tissue which is quantified in the contrast-to-tissue ratio. Important application areas for contrast agents are the enhancement of hypo-echoic regions, perfusion imaging, and functional assessment of, for example, the myocardium[1].

In non-destructive contrast agent imaging, the peak transmitted acoustic pressure is limited by the destruction threshold of the contrast agent. This threshold is usually much lower than the maximum allowed mechanical index (MI) which limits the

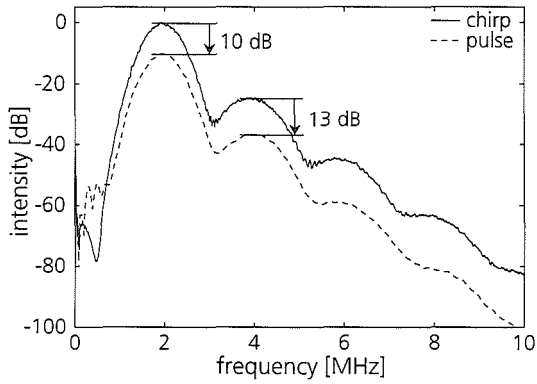

Figure 4.1: Simulated response of 7000 contrast agent bubbles randomly distributed in space with SonoVue size distribution excited with chirp (—) and pulse (---) with equal centre frequency (2 MHz), bandwidth (45%), and peak amplitude (50 kPa).

peak transmitted pressure to avoid cavitation and tissue damage[13]. Therefore, non-destructive contrast agent imaging is more severely limited in transmitted peak amplitude and produces images with lower SNR than conventional imaging and tissue harmonic imaging. To improve the SNR in contrast agent imaging, one can either lower the noise level or increase the signal level. The noise level is mainly fixed by system design. Increasing the signal level by increasing the transmission amplitude is limited by the bubble destruction threshold. Coded excitation can be applied to increase the signal energy without increasing the peak transmitted amplitude by using longer pulses and compression on receive.

Previously, we reported in a simulation study that showed that chirp excitation can increase the relative level of second harmonic over pulse excitation, which potentially results in improved CTR[3]. The main result from this study is summarised in Fig. 4.1 which shows in frequency domain the simulated response of 7000 bubbles randomly distributed in space and with SonoVue™ size distribution to a pulse and a chirp having equal centre frequency (2 MHz), bandwidth (45%) and peak amplitude (50 kPa). It is clear that apart from an energy difference of 10 dB between pulse and chirp which explains the difference between the curves at the fundamental, there is an additional difference of approximately 3 dB at the second harmonic. This effect reflects the increased radial excursion of the contrast agent bubbles due to the longer length of the chirp and theoretically improves the CTR by the same amount.

In this paper we propose a chirp excitation method with a non-linear decoder for use with contrast agent imaging. Firstly, results from the non-linear decoder on simulated bubble echoes will be examined. Secondly, the non-linear chirp compression method is evaluated using measured reflections from a flat plate reflector that contain

harmonics from non-linear propagation. Finally, in-vitro B-scan images using pulse and chirp excitations are compared to test the performance of the non-linear compression technique in-vitro and to indicate the current limitations of this technique.

4.2 THEORY

Chirp excitation operates by transmission of a long frequency modulated burst into the medium. The main design parameters of a chirp are its length and its bandwidth, which determine the energy contained in the chirp and the obtainable axial resolution after compression, respectively. An additional apodisation window can be used to lower the side-lobe levels that are inherent to compression. After reception of the echo signal, a compression filter removes the coding and recovers the axial resolution that was disturbed during the coding process. Conventionally, chirp compression takes a matched filter approach in which an autocorrelation filter with an impulse response that is the time inverse of the transmitted chirp is used. As the compression filter has the same bandwidth as the fundamental of the transmitted chirp, this is equivalent to extracting the fundamental from the echo signal and adjusting the phase of the frequency components.

We propose a non-linear compression filter that can selectively extract and compress the second harmonic from the received echo. Figure 4.2 shows a schematic overview of the compression method. The first part is equal to the setup for regular chirp imaging: a chirp containing only the fundamental is sent into a non-linear medium. The medium (the patient in clinical situations) generates an echo that contains both the fundamental and higher harmonics. Instead of using a matched filter based on the time inverse of the transmitted chirp as its impulse response, we defined a compression filter that, compared to a regular compression filter, has twice the instantaneous frequency at every time point. In addition, the apodisation was changed to obtain the same bandwidth as we would get from frequency doubling the pulse that was used as excitation. For example, if the excitation chirp ranges between 2 MHz and 4 MHz, the compression filter will range between 4 MHz and 8 MHz. In frequency domain this design is equivalent to a compression filter that extracts and compresses the second harmonic from the echo signal. The compressed echo has good axial resolution and a centre frequency at the second harmonic of the transmitted chirp.

To compare regular pulse excitation which uses short pulses with large bandwidth and chirp excitation which uses long bursts with large bandwidth, we designed a Gaussian envelope pulse and a Gaussian apodised chirp that have the same Fourier magnitude spectrum. Figure 4.3 shows the pulse and the chirp in time and frequency domain that were used as excitation in the simulation study and the in-vitro validation. Centre frequency and bandwidth of both pulses are 2 MHz and 45% respectively. The −6 dB length is 2.0 μs for the pulse and 9.4 μs for the chirp. When both pulses are scaled to equal peak amplitude, the energy difference between the pulse and the chirp is 10 dB.

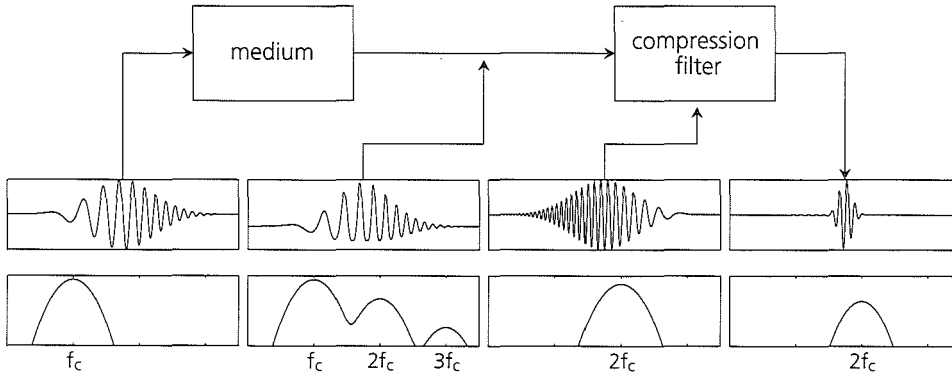

Figure 4.2: Schematic diagram of harmonic chirp compression method for selective compression and extraction of second harmonic part from received response

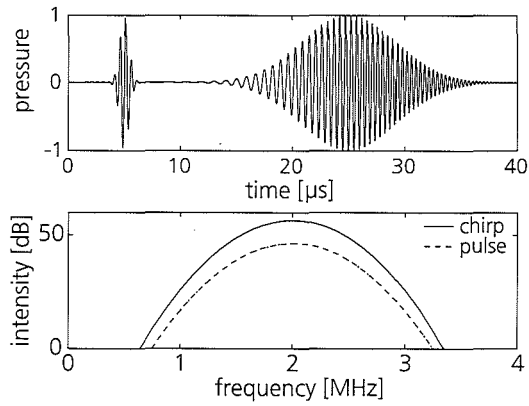

Figure 4.3: Gaussian pulse and linear, Gaussian apodised chirp with equal centre frequency, bandwidth and equal Fourier magnitude spectra that were used as excitation in simulation study and experimental validation.

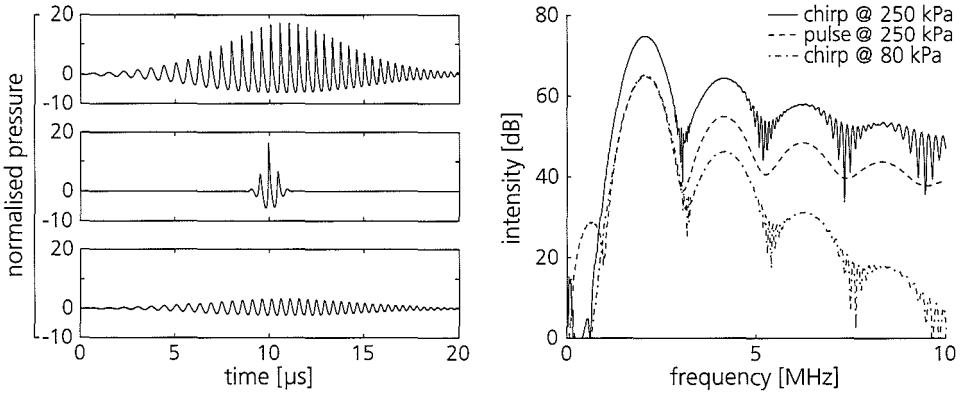

Figure 4.4: Simulated non-linear propagation from KZK-equation using pulse and chirp having either equal peak amplitude or equal energy. Equal peak amplitude excitations generate equal relative levels of harmonics, while equal energy chirp generates fewer harmonics than pulse.

Previous research has shown that the level of tissue harmonics due to non-linear propagation, depends, other variables being equal, on peak pressure but not on pulse energy. Figure 4.4 shows simulation results obtained from solving the KZK-equation, which models the effect of non-linear propagation, diffraction and attenuation[26], in time domain for a focussed 25 mm diameter transducer with 75 mm focal length using pulse and chirp having either equal peak pressure (250 kPa) or equal signal energy (250 kPa pulse and 80 kPa chirp). The curves show the simulated responses at focal depth. It is clear that a chirp produces significantly less harmonics than an equal energy pulse, while equal peak amplitude excitations produce relative levels of harmonics that are approximately equal. This effect is explained by the fact that generation of propagation harmonics only accumulates over propagation depth and not over pulse duration. The response from bubbles, however, depends on both peak amplitude and pulse length. As bubble dynamics can be approximately described by a damped mass-spring system, effects of the excitation signal accumulate over pulse length, especially around the resonance frequency of the bubble.

For contrast agent bubbles the generation of harmonics is mainly dependent on peak bubble wall excursion[2]. Simulations have shown that chirp excitation causes larger bubble wall excursion than an equal amplitude pulse. Measurements on 2-D-images obtained with an optical 25 MHz fast framing camera system[10] are in agreement with the simulation results. Figure 4.5 shows radius-time curves of a 3.8 μm diameter contrast agent bubble recorded at 11.5 million frames per second as a function of time with the corresponding Fourier transform when subsequently excited with a pulse and a chirp with 2 MHz centre frequency and 45% bandwidth at approximately 120 kPa peak pressure. The figure clearly shows that the peak bubble wall excursion

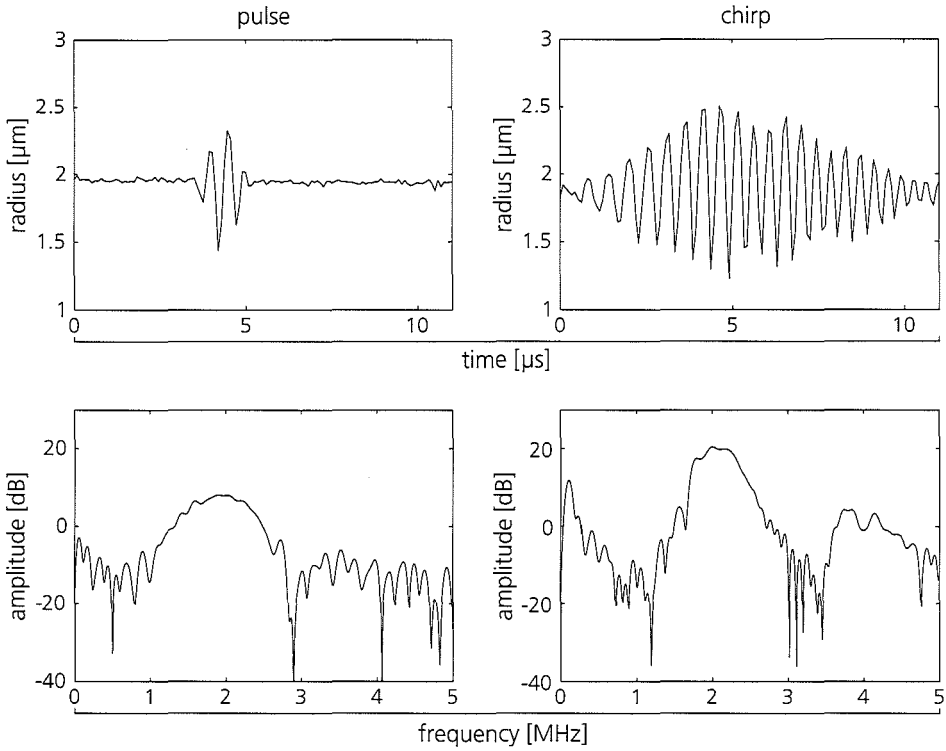

Figure 4.5: Radial response of 3.8 μm diameter contrast agent bubble as observed with Brandaris-128 fast framing camera at 11.5 million frames per second. The radial excursion is clearly larger for chirp than for pulse.

is larger for chirp excitation than for pulse excitation. The Fourier transform clearly shows a difference in energy at the fundamental of 10 dB. The second harmonic is visible for the chirp; however, poor SNR in the pulse response masked the second harmonic component.

To calculate the radius of a contrast agent bubble as a function of time when exposed to these excitation waveforms, we used an RPNNP differential equation which is named after its developers Rayleigh, Plesset, Noltingk, Neppiras and Poritski. The RPNNP equation, which describes the radial oscillations of an ideal gas bubble under time varying acoustic pressure, was modified to include the effects of an additional restoring force due to shell stiffness and friction inside the shell[15]. A computer program was developed in Matlab (The Mathworks, Inc., Natick, MA, USA) and C to solve the equation for a given excitation signal using a fifth order Runge-Kutta algorithm with variable step size[35]. With the simulation program we investigated the

effect of different excitation signals on the generation of harmonics from contrast agent bubbles.

4.3 METHOD

The harmonic chirp imaging method, including the compression, was initially evaluated on simulated bubble echo signals and measured propagation harmonics. We simulated the echoes generated from 1.85 μm, 2.75 μm, and 4.50 μm radius contrast agent bubbles with SonoVue parameters[21]. At these sizes the resonance frequencies of the bubbles are 3.5 MHz, 2 MHz, and 1 MHz respectively. Thus the bubbles are driven below, at and above their resonance frequencies for the given excitations. As excitation we used the 2 MHz centre frequency pulse and chirp as defined in Fig. 4.3 and scaled to 150 kPa peak pressure.

In addition, we measured reflections from a flat steel reflector that was positioned at 75 mm from a 3.5 MHz, 65% bandwidth unfocussed, 12 mm diameter single element transducer (Imasonic, Besançon, France) in pulse-echo mode using the aforementioned pulse and chirp at approximately 1 MPa peak pressure. The excitations were generated with an arbitrary waveform generator (LW420A, LeCroy, Chestnut Ridge, NY ,USA) and amplified by a 50 dB linear power amplifier (2100L, ENI, Rochester, USA). The amplitude was adjusted with a variable attenuator (355C/D, HP, Palo Alto, CA, USA). The simulated and measured echoes were either filtered in case of pulse echo or compressed in case of chirp echo to extract the fundamental and the second harmonic. The resulting signals were envelope detected and compared on the basis of axial resolution and side-lobe level.

To evaluate the performance of the non-linear compression technique in-vitro, we obtained B-mode images by mechanically scanning over a flow phantom using the pulse and chirp excitations as defined in Fig. 4.3 in fundamental and second harmonic mode. The flow phantom consisted of 2% agar-agar gel with 0.4% carborundum particles to mimic tissue scattering. Embedded in the phantom were two flow channels of 10 mm and 5 mm diameter in which an experimental contrast agent (BR14, Bracco Research SA, Geneva, Switzerland) in 1:2,000 dilution was flowing. The flow channels were slightly angled relative to the incident ultrasound field to prevent specular reflections from the flow channel boundaries. The flow was maintained by a gear pump (GA-X21, Micropump Ltd., St Neots, Cambridgeshire, UK) at approximately 0.6 $^{m}/_{s}$.

The phantom was mounted on a hand-operated x–y table and translated relative to a fixed transducer to make the B-scan images. The transducer was the 3.5 MHz single element transducer. Both excitations were hydrophone calibrated to have equal peak amplitudes up to MI=0.2. B-mode images were obtained by scanning the phantom by increments of 0.5 mm under the fixed transducer. The scanning direction was perpendicular to the direction of the flow. At each scanning position, the resulting echo was digitised and recorded with a LeCroy digital oscilloscope. The images were

Table 4.1: Fundamental and second harmonic axial resolution (mm) obtained for simulated 1.85 μm, 2.75 μm, and 4.50 μm radius single bubble responses using pulse and chirp excitations

	1.85 μm radius		2.75 μm radius		4.50 μm radius	
	fundamental	2nd harm.	fundamental	2nd harm.	fundamental	2nd harm.
pulse	2.1	1.8	2.7	2.1	2.0	1.7
chirp	2.1	1.9	2.7	2.3	2.0	1.8

processed off-line on an IBM-compatible PC.

The performance of the non-linear chirp compression technique was evaluated by comparing the apparent sizes of the flow channels in the chirp images to the sizes in the images made by conventional pulsed imaging. In addition, the tissue SNR levels are compared to quantify the differences between the two excitation methods. To obtain the tissue signal levels, appropriate regions in the images were selected and averaged. The noise level was determined from a separate noise measurement by using the entire system without generating an excitation signal.

4.4 RESULTS

The envelope detected fundamental and second harmonic parts of the calculated bubble response are shown in Fig. 4.6 for each bubble size excited with either pulse or chirp. The ordinates are shown on a log scale to visualise of the side-lobes from chirp compression. Apart from the differences in peak energy level of the main lobes in each figure, the main lobes look similar in shape. Table 4.1 shows the obtained axial resolution for each of the curves in Fig. 4.6. From this table we see that the axial resolution is in all cases comparable, with only a very slight degradation for the bubble at resonance. However, the detected envelopes from chirp excitation exhibit range side-lobes as was expected from the use of a compression filter. The side-lobe levels are all more than 50 dB below the main lobe.

Experimental results from the compression of chirp echoes from the flat plate are shown in Fig. 4.7. On logarithmic scale, this figure shows the envelope detected signal using the linear and nonlinear compression filters on the echoes reflected by the flat plate generated by the pulse and chirp excitations. Table 4.2 quantifies axial resolutions for these measurements. We see that as with the simulated bubble echoes, the curves from pulse and chirp look very similar. Axial resolutions, therefore, are comparable, which can be seen from the table as well. Side-lobe levels can bee seen to 60 dB and 30 dB below the main lobe for the linear and nonlinear compression filters, respectively.

Figure 4.8 shows the B-mode images of the 10 mm (a) and 5 mm (b) flow channels

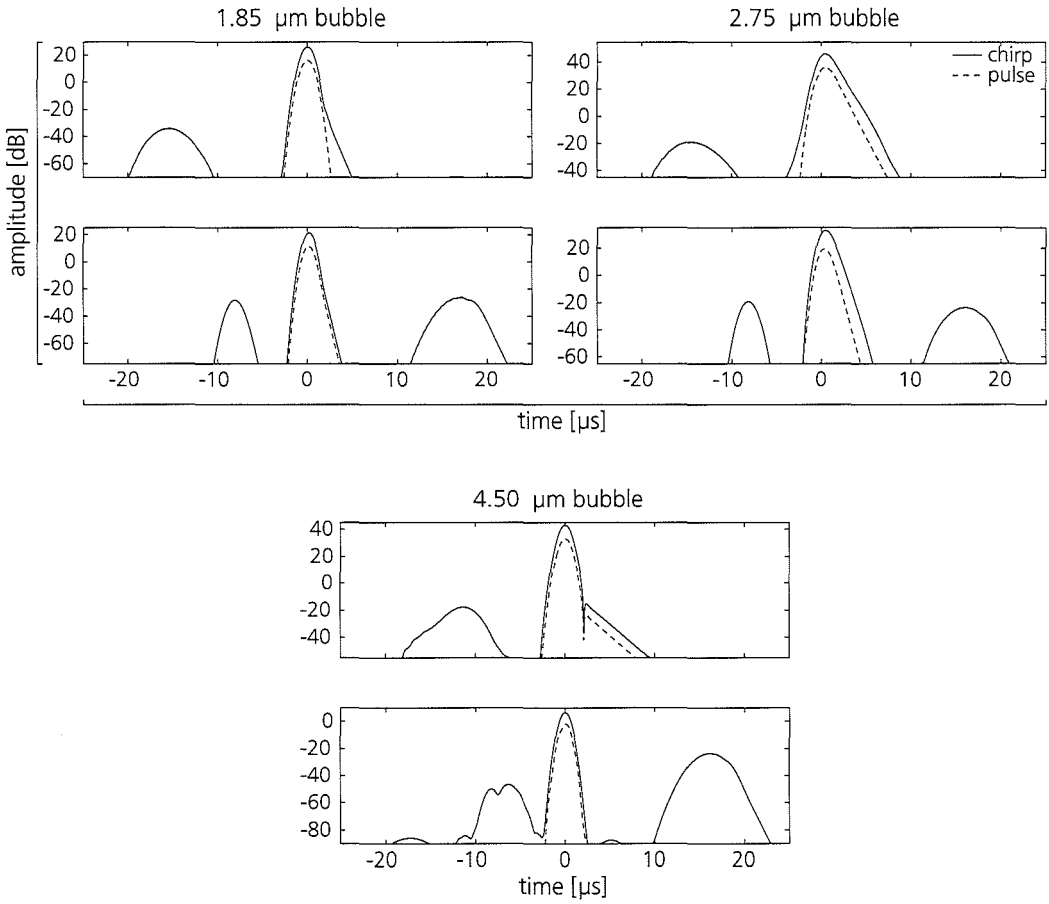

Figure 4.6: Envelope detected fundamental and second harmonic responses of simulated 1.85 μm, 2.75 μm, and 4.50 μm radius bubbles excited with pulse and chirp.

Table 4.2: Fundamental and second harmonic axial resolution (mm) for flat plate reflector using pulse and chirp excitations.

	fundamental	2nd harm.
pulse	2.0	1.8
chirp	2.2	1.9

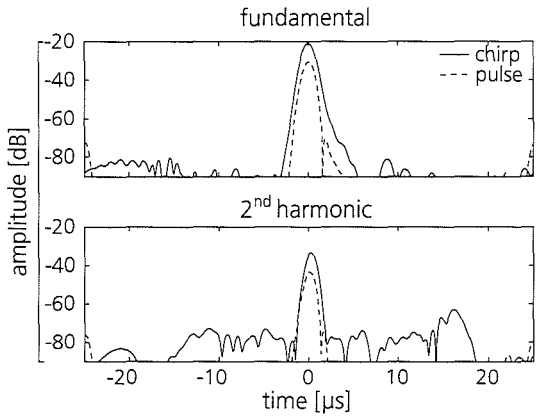

Figure 4.7: Envelope detected fundamental and second harmonic of measured non-linear propagation harmonics using pulse and chirp excitations.

embedded in the phantom as obtained with a single element transducer in pulse-echo mode. The top row shows images from pulse and chirp in fundamental mode, the bottom row images in harmonic mode. The dynamic range in all images is 40 dB and all images are normalised to give good contrast between the flow channel and surrounding tissue mimicking material. In all images the flow channel is clearly visible as an echogenic region. However, shadowing below the flow channels was visible which may be caused by accumulation of contrast agent due to floatation. The apparent channel size agrees reasonably well between pulse and chirp excitation images in the same imaging mode. However, in the chirp harmonic images side-lobes are visible as shadows above and below the flow channel. Speckle is well developed in the fundamental images, with the pulse images being slightly noisier due to the lower signal energy in the pulse excitation. The harmonic images suffer from relatively low SNR due to the low transmitted amplitude to decrease the generation of contaminating tissue harmonics. There is, however, some speckle visible through the noise for the chirp harmonic images, indicating the advantage of chirp excitation for harmonic images as well.

Table 4.3 shows tissue SNR and the sizes of the flow channels as measured from the images in axial direction. The SNR value for pulse harmonic image could not be calculated as the image is too noisy to calculate a tissue signal. However, estimating this value from the SNR obtained from the chirp harmonic image, we estimate it to be lower than 0 dB. An increase of approximately 10 dB in SNR was found for chirp excitation compared to pulse excitation. The size of the flow channels is overestimated in all images. In fundamental mode, the imaged size of the flow channel agrees. For harmonic mode there is a slight increase in measured flow channel size for chirp.

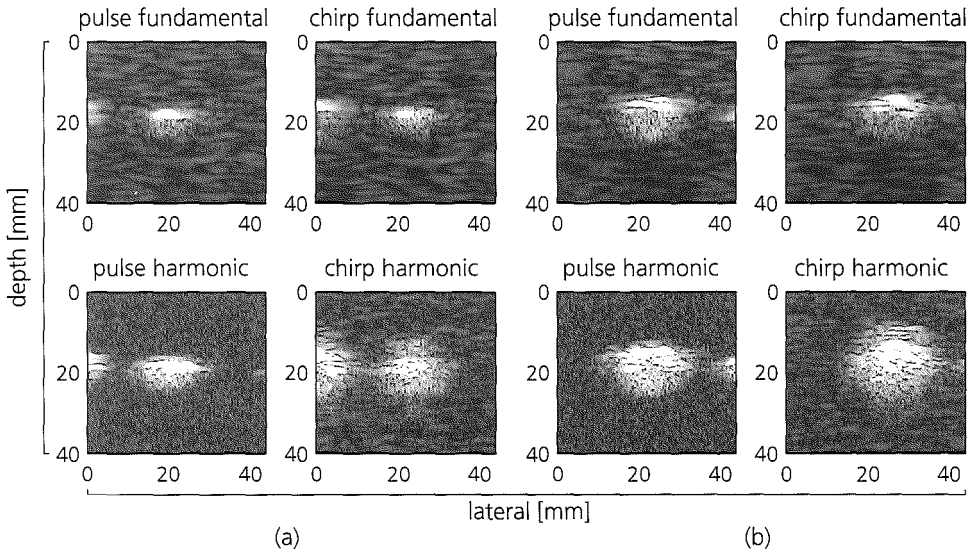

Figure 4.8: In vitro B-mode images of flow phantom with embedded 5 mm (a) and 10 mm (b) flow channels containing contrast agent using pulse and chirp excitation displayed at 40 dB dynamic range.

Table 4.3: SNR and flow channel sizes from B-mode images for pulse and chirp excitations in fundamental and second harmonic imaging mode.

	pulse		chirp	
	fundamental	2^{nd} harm.	fundamental	2^{nd} harm.
SNR	19.3 dB	< 0 dB	30.1 dB	8.0 dB
5 mm channel	8 mm	9 mm	8 mm	10 mm
10 mm channel	12 mm	14 mm	12 mm	15 mm

4.5 DISCUSSION

The use of chirp excitation signals is critically dependent on the performance of the compression filter to obtain a narrow main lobe and low range side-lobe levels. This becomes even more important when designing a compression filter for compression of harmonic signals. For good compression performance, the phase relations between the individual frequency components in the echo signal that is the input for the compression filter must be known when designing the compression filter. In a linear system this is the case as in those systems the change in phase relations is dependent only on the system itself, i.e. not on the phase relations in the signal that is input into the system. For the non-linear case this may not hold as frequency components are generated that are not in the input signal and hence may have arbitrary phase relations which prevent adequate compression.

The non-linear compression filter has shown to adequately compress simulated bubble echoes and measured propagation harmonics. Axial resolutions after compression are within 10% of the axial resolutions obtained from regular pulse excitation. Side-lobe levels are at least 30 dB below the main lobe for compressed simulated single bubble responses and compressed propagation harmonics, except for the 4.50 μm bubble in harmonic mode. Although these side-lobe levels may create visible ghost or blooming artefacts, they may be tolerable in cases where sensitive detection of contrast agent is wanted.

By design, an increase of 10 dB in SNR for B-mode images obtained from chirp excitation over pulse excitation in both fundamental and harmonic mode was expected. This improvement is found in the chirp fundamental image and qualitatively observed in the chirp harmonic image although the SNR for the pulse harmonic image cannot be quantified. Imaged size of the flow channel was found to be approximately equal when comparing the pulse fundamental images with the chirp fundamental images and 10% worse when comparing the chirp harmonic images with the pulse harmonic images. CTR was expected to increase approximately 2 dB in the chirp harmonic images compared to the pulse harmonic images. In the images, however, the CTR was found to decrease 1 dB between chirp harmonic and pulse harmonic. This value was degraded by the fact that tissue signal is lower than noise in the pulse harmonic image. Actual improvement in CTR can hopefully be demonstrated in future studies where noise level is reduced by, for example, averaging. Therefore, we consider the 1 dB decrease in CTR a lower bound on the actual CTR difference in the images. Additionally, we clearly see that the speckle patterns of pulse fundamental images and chirp fundamental images are highly comparable, indicating a high similarity in the total response of imaging system and therefore, axial resolution, although much different excitations are used. However, significant side-lobes were seen in the chirp harmonic images. Although the side-lobes at the top of the flow channel are probably exaggerated due to accumulation of contrast agent at the top of the flow channel that was observed during the experiments, this still indicates difficulties with either the matching of the compression filter to the transmitted chirp or a more

fundamental difference in chirp harmonics generation for bubbles.

In conclusion, chirp excitation with a non-linear decoder has been shown to produce images with resolution comparable to pulse excitation. However, improvement in the suppression of compression artefacts, i.e. range side-lobes, is needed.

5 COMPARING BUBBLE DESTRUCTION INDUCED BY PULSE AND CHIRP EXCITATIONS

ABSTRACT

Ultrasound imaging has experienced significant progress with the introduction of gas microbubbles as contrast agent (CA). Since a few years, ultrasound contrast agents are now used in a variety of applications in radiology and cardiology. Due to the unique acoustic properties of microbubbles, new imaging methods have been developed and are used for contrast imaging as well as for tissue imaging. Most recent contrast imaging methods are based on very low insonification levels in order to avoid tissue echoes but mainly microbubble destruction. Because microbubble destruction correlates positively with transmitted waveform amplitude and length, short bursts with low acoustic pressures are usually preferred. Recently, we have proposed a new imaging method based on coded excitation. Although coded excitation provides a higher signal to noise ratio compared to standard transmit signals, microbubble destruction is likely to be critical compared to non-coded waveforms since coded excitation uses long transmit waveforms. In a continuation of our previous work, we explored in this study the destruction of contrast microbubbles when insonified with a chirp signal at 1.7 MHz and 45% bandwidth using in-vitro acoustic measurements. Moreover, we compared the destruction rate caused by a chirp excitation to the destruction rate produced by pulsed wave with the same frequency bandwidth and amplitude. To evaluate the destruction rate, the microbubbles were insonified with separate transducer transmitting a low acoustic pressure pulse before and after insonification with the destruction signal. The transducer had a 3.5 MHz center frequency and transmitted a pulse of 2.5 MHz and 45% relative bandwidth. The destruction was quantified by correlating contrast responses before and after destruction. The acoustic measurements demonstrated that for acoustic pressures up to 400 kPa, chirp and pulse did not produce significant bubble destruction, which was demonstrated by a high correlation coefficient. Above this acoustic threshold, the chirp wave affects the bubbles considerably especially at very high pressures as translated by the low correlation coefficient. In conclusion, for acoustic pressures that are currently in use for contrast imaging, the

chirp increases the contrast signal in addition to being considered as a non-destructive wave.

This chapter is based on the manuscript: A. Bouakaz, J.M.G. Borsboom, and N. de Jong. Comparison of contrast agent destruction induced by pulse and chirp excitations. *To be submitted.*

5.1 INTRODUCTION

Ultrasound contrast agents (UCA) are now commercially available in Europe, Japan and the United States. They are approved and used for left ventricular opacification and for enhanced endocardial border delineation. The first generations of contrast agents were composed of free air bubbles whereas newer generations contain less-diffusable gas cores with very flexible and soft envelopes[20]. The new processes in bubble design have improved microbubble persistence significantly. The availability of newer generations has stimulated many new imaging methods as well as applications. The new imaging methods are based on the unique acoustical signatures of gas microbubbles, which differ from the signatures of tissue[14]. One of these properties is harmonic scattering[15] although it has been used for a while ago for bubble detection and sizing[29]. This nonlinear property has been used to selectively image contrast bubbles and is now the basis of a new imaging method employed in commercial systems for Transthorasic imaging and termed contrast harmonic imaging. It is based on the difference in nonlinear scattering properties between gas microbubbles and tissues mainly at the second harmonic frequency. This is now successfully exploited due to improved lifetime and improved physical properties of the agents. Extensive research has been carried on the nonlinear behavior of microbubbles in an ultrasound field. Since then this has lead to the development of new imaging methods based on the harmonic scattering properties of gas bubbles. Methods such as pulse inversion, power modulation, which are commercially available contrast imaging methods take advantage of the nonlinear properties of contrast microbubbles, and have shown success in various applications such as LVO but have shown limited success in for example detecting myocardial perfusion during echocardiographic examinations with 'difficult-to-image' patients. Hence new imaging methods are investigated based on the unique acoustic properties of gas microbubbles[39, 4]. One of the main limitations of current linear or nonlinear contrast imaging methods is the strong echo produced by the tissue itself. While increasing the applied acoustic pressure increases the nonlinear scattering of microbubbles, it causes microbubble destruction in addition to the creation of tissue harmonic components, which will ultimately contaminate the contrast harmonics. This has lead to the utilization of very low transmit pressures (low mechanical index (MI)) to avoid microbubbles and tissue harmonics. Although new low-MI methods have proven to perform successfully in various applications, they still suffer in many circumstances from low signal levels in for example perfusion estimation where only a small amount of microbubbles is present. The ultimate perfusion technique should be

able to ascertain the suppression of the strong (linear or nonlinear) tissue echoes while increasing the bubble echoes. The discrimination between non-perfused tissue and microbubble-perfused tissue is usually termed contrast-to-tissue ratio (CTR). In order to ensure a high CTR, microbubble destruction due to ultrasound should be avoided in default of being minimized.

Recently we have suggested a new nonlinear imaging method for contrast agent based on coded excitations[3]. The method consisted of transmitting a chirp of 2 MHz center frequency and 45% bandwidth and the results were compared to a transmission of a Gaussian pulse with equal bandwidth and frequency. We have shown that for acoustic pressure up to 300 kPa, an increase in signal to noise ratio of up to 13 dB was achieved with chirp compared to pulse insonification while axial resolution was comparable in both situations. However to construct a chirp with the required characteristics, the total length of the chirped signal was almost 10 μs. Since long transmit signals are usually not used in contrast imaging to avoid microbubble destruction (and poor axial resolution), it is likely that microbubble destruction using chirps to be of concern. Therefore we sought in this study to evaluate the destruction rate with chirp excitation and compare it to pulsed excitation case.

5.2 METHOD AND EXPERIMENTAL SETUP

To compare the difference in destructivity of pulse, burst and chirp excitations, we performed water tank measurements on BR14 contrast agent. A small, acoustically transparent container was filled with a 1:5000 dilution of BR14 and placed at the confocal point of two perpendicularly mounted broadband transducers as shown in Fig. 5.1. The transducer used for transmission was a 32 mm diameter, PZT transducer with 2.25 MHz centre frequency and 75 mm focal length (Panametrics, Waltham, MA, USA). The scattered echo signal was received with an unfocussed, 15 mm diameter composite transducer with 3.5 MHz centre frequency (Imasonic SA, Besançon, France). Excitation sequences were generated with a two-channel arbitrary waveform generator (LW420A, LeCroy, Chestnut Ridge, NY, USA) and amplified with a 60 dB linear power amplifier (A-500, ENI, Rochester, USA). The amplitude was adjusted with two variable attenuators (355C/D, HP, Palo Alto, CA, USA and 50TX102, Alan Industries, Columbus, IN, USA). Excitation pressure levels were measured separately with a calibrated PVDF needle hydrophone (Precision Acoustics Ltd., Dorchester, UK) in gas saturated water. The received echo signal was amplified with a broadband preamplifier (AU-3A-0110, Miteq, Hauppage, NY, USA), digitised with an 8-bit digital oscilloscope (9400A, LeCroy, Chestnut Ridge, NY, USA), and recorded on a personal computer through an IEEE 488 interface.

The excitation sequence for the measurements is shown in Fig. 5.2. The sequence starts with an interrogation pulse consisting of a 10 cycle, 2.5 MHz burst with a peak negative pressure of 34 kPa (MI=0.02). This pressure is low enough not to disrupt the bubbles, while obtaining acceptable signal-to-noise ratio in the measurements. An

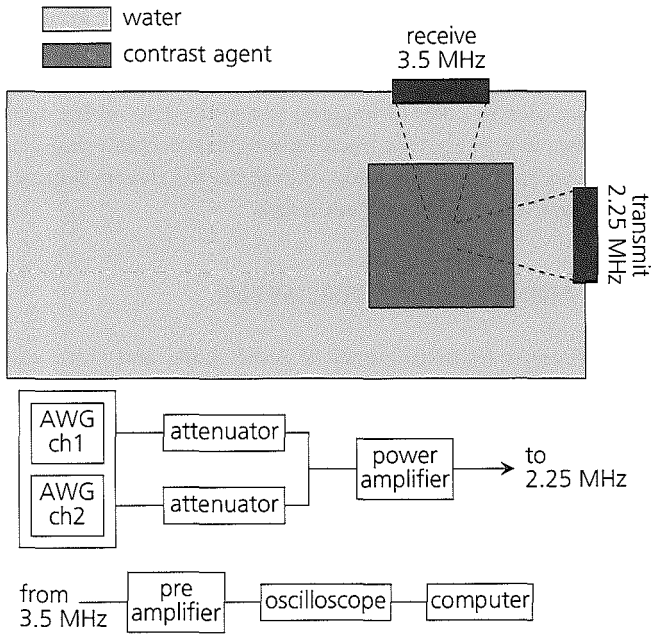

Figure 5.1: Schematic setup for contrast agent destruction measurements.

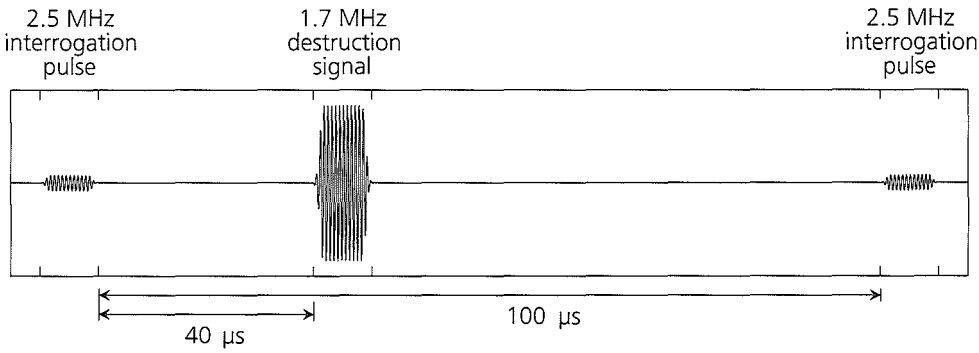

Figure 5.2: Excitation sequence for bubble destruction measurements using pulse, burst and chirp destruction signals.

equal interrogation pulse at 100 μs from the first one was applied to track changes in the contrast agent bubbles in the targeted region. In between the two interrogation pulses, a destructing excitation signal was applied at various peak pressure levels at 40 μs from the first interrogation pulse. The destruction signal consisted of a 10 cycle burst, a 45% relative bandwidth, Gaussian apodised pulse, or a 10 μs, 45% relative bandwidth, Gaussian apodised quadratic chirp, all at 1.7 MHz centre frequency. The pulse and chirp were chosen so that their normalised Fourier magnitude spectra were equal. The peak negative pressure of the destruction signals was varied between 11 kPa (MI=0.009) and 1.6 MPa (MI=1.23). The centre frequencies of the interrogation pulses and the destruction signals were chosen differently to allow for filtering out the destruction signal. Initial measurements had shown that at high destruction pressures, the destruction pulse was producing a long trace of secondary echoes after the first echo from passing through the contrast agent and, hence, obscuring the echo from the second interrogation pulse. By using different frequencies we could us a band pass filter to extract the echoes from the interrogation pulses at 2.5 MHz and suppress the destruction signals and their second harmonics at 1.7 MHz and 3.4 MHz. Although with this pulse sequence we optimally destroy a different set of bubbles than we can optimally detect, we think that a change in a bubble in the target region will change the response, even when we detect it with an off resonance burst.

Figure 5.3 shows some examples of received echo signals. The top two figures show the received pulse sequence for a low amplitude pulse or chirp destruction signal. Although both the pulse and chirp have equal peak power levels, it is evident from the higher echo signal level of the destruction signal that the chirp destruction signal contains more energy. Furthermore, the two interrogation pulses before and after the destruction signal look similar which is an indication that the contrast agent bubbles present in the target region have not changed significantly by the destruction signal.

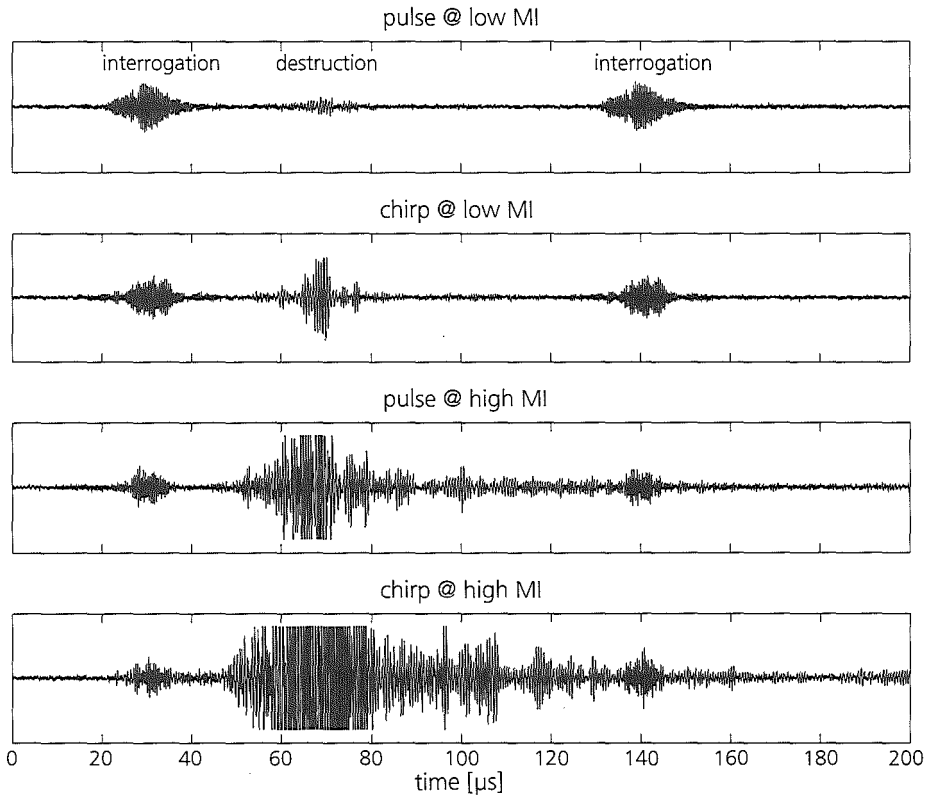

Figure 5.3: Example of traces received for pulse and chirp destruction signals at low (top figures) and high MI (bottom figures).

Any difference that is visible is due to noise. The bottom two figures show an example of received echo signals for high amplitude pulse and chirp destruction signals. As the echo from the destruction signal was not necessary for processing, its echo was limited on recording. At these destruction pressures, the echoes from interrogation pulses were different, although this is not very clear in the example traces. Clearly visible are the secondary echoes from the destruction signal that overlap the second interrogation pulse.

At each destruction pressure and for each destruction signal, 100 echo traces were recorded and digitally with a band pass filter with centre frequency 2.5 MHz and 10% fractional bandwidth. Subsequently, for each trace the two interrogation echoes were windowed with a 40 μs rectangular window and correlated. We used correlation as the measure of change as it is sensitive to phase changes in the signal which, for example,

integrated power is not. We expect that a change in the contrast bubble induced by the destruction signal will produce a change in both the amplitude and the phase of the received echo. Finally, the correlations of the traces were averaged using the Fisher-Z transform.

5.3 RESULTS AND DISCUSSION

Figure 5.4 displays an example of a measured traces after the filtering operation. The upper panel shows the filtered signals from the contrast microbubbles before (1) and after (2) insonification with a 64 kPa amplitude chirp. The responses of the microbubbles before and after exposure to the chirp signal are very similar indicating no or minimal destruction of the contrast microbubbles with the chirp at this applied acoustic pressure. The correlation coefficient of both responses as a function of the alignment of the two 40 μs windows, as given in the lower panel by the solid line, has a high maximum value indicative of little change between both signals. Moreover, the curve is single peaked and decays rapidly for increasing misalignment of the two windows which is an indication that we appropriately use correlation as a measure of change between the echoes from the interrogation pulses. The same panel shows the correlation for a chirp signal with a higher acoustic amplitude (1.1 MPa). The dashed curve has a maximum amplitude of 0.77 indicative of a change in the microbubble response after being interrogated with the chirp signal. Finally, the dash-dotted curve in the lower panel shows the correlation curve for a 1.1 MPa pulse with a maximum correlation of 0.92. Although the chirp appeared to be destructive to the microbubbles, the pulse with same acoustic amplitude seemed to have less influence on the response of the microbubbles.

The results obtained at different acoustic pressures for both the pulse and chirp signals are summarized in Fig. 5.5. The correlation coefficient of the responses before and after the destructive signal is calculated for the pulse (—) and the chirp (-·-·) and for each applied acoustic pressure. The figure shows also the result obtained when the contrast microbubbles are interrogated with a burst signal (---) which has the same length as the chirp signal. The curves demonstrate that for acoustic pressures up to 400 kPa, the chirp signal has minimal consequence on the contrast microbubbles as revealed by the correlation coefficient level. Within this pressure range, we can consider that transmissions of a chirp signal will not cause any effects on the bubbles. However, for acoustic pressures higher than 500 kPa, the chirp signal clearly influences response of the bubbles as indicated by the correlation coefficient. Although the pulse and the burst waveforms also cause some bubble destruction, it is clear that the chirp has more affect on the contrast causing therefore reduction in the return signal.

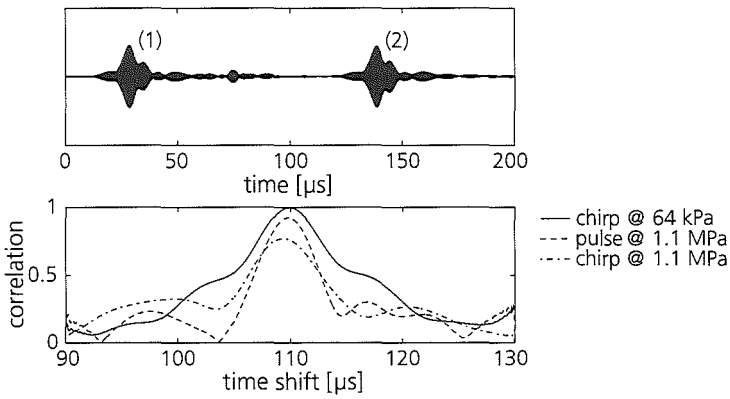

Figure 5.4: Example of a filtered trace and correlations for low MI chirp, high MI pulse and high MI chirp. The upper panel shows the filtered signals from the contrast microbubbles before (1) and after (2) insonification with a 64 kPa amplitude chirp. The lower panel shows the envelope of the correlation coefficient as a function of the alignment of the two correlation windows.

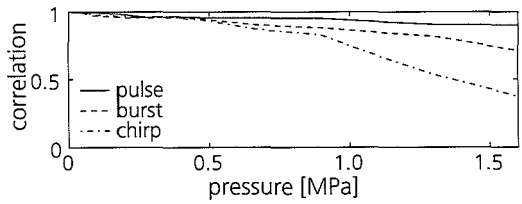

Figure 5.5: Correlation as a function of destruction pressure for pulse (—), burst (---) and chirp (-·--).

5.4 CONCLUSION

Chirped waveforms have been proposed in the past to increase the signal to noise ratio for fundamental tissue imaging. We have recently suggested utilizing the chirps to increase the scattered signals from contrast microbubbles for harmonic imaging. Simulations and in-vitro acoustic measurements have demonstrated an increase of 10 dB in the second harmonic signal from the microbubbles using chirps compared to pulse waveforms of the same amplitude and frequency bandwidth. However since chirps consist of rather long signals, microbubble destruction with chirps might be higher than with pulsed waves. It is within that context that we investigated in this paper the affect that has a chirp signal on contrast microbubbles and on their acoustic response. By transmitting a chirp signal of 1.7 MHz, the experimental results proved that below acoustic pressures of 400 kPa, chirp transmissions have no or minimal influences on the contrast response, indicating that chirps can be used to image contrast microbubbles in a non-destructive mode. Above this acoustic threshold, chirps have shown to provoke more change in the response of the bubble than pulsed waves, which is translated by a reduction in the amplitude of the scattered signal. In conclusion, chirps waveforms with appropriate acoustic pressure can be used to increase the signal to noise ratio at the fundamental and harmonic frequency while maintaining the bubbles shape and response unaffected.

We should indicate however that our experimental procedure is a little different than current imaging procedures in terms of firing sequences. In our in-vitro measurements, the microbubbles are interrogated 100 times with a sequence of low MI pulse –destruction signal– low MI pulse and the final result is an average of the 100 recordings. In standard imaging modes, the bubbles will be irradiated sequentially for a number of times and therefore would not have enough time to refresh the target zone since there is a cumulative destruction effect. As a consequence, we would expect more destruction than when using our experimental procedure. Nevertheless, since the same experimental procedure is used for both chirp and pulse excitation, the final result would not be influenced and our conclusion is still valid in this case.

6 CONTRAST IMAGING USING DUAL FREQUENCY EXPOSURE

ABSTRACT

In this study, we present a new imaging method that is capable of detecting echoes from microbubbles and eliminate echoes emanating from non-oscillating structures like tissue. The method is based on simultaneous insonation of a contrast agent bubble with a low (LF) and a high (HF) frequency signal. The LF signal is used to induce size changes in the microbubble by the compression and the rarefaction phases. During these phases of the LF signal, a HF signal is transmitted to image the microbubbles. Hence, the HF signal will probe the same bubble but at different stages of its oscillation cycle: small and large. Simulations were performed using a modified Herring equation using a single cycle at 0.5 MHz and seven cycles at 3.5 MHz. The results show that by incorporating the LF signal, the bubbles respond differently compared to single frequency excitation. In addition, we obtained optical recordings of contrast agent microbubbles with the Brandaris-128 high-speed camera system. Two transducers were used that transmitted the 0.5 MHz and 3.5 MHz signals. The recordings consisted of 128 successive frames obtained at a frame rate of 14 MHz. A Sonovue™ microbubble of 4 μm diameter was observed oscillating under the effects of both LF and HF signals. The optical recordings show that, depending on the phase of the LF signal, the bubble response at 3.5 MHz changes significantly. A larger response is obtained at the compression phase when compared to the response at the expansion phase. The decorrelation between the signals from the compression and expansion phases of the LF signal is sufficiently high to be used as a parameter to detect contrast microbubbles and discriminate them from tissue. In conclusion, these preliminary results demonstrate the feasibility of this approach in improving contrast agent detection.

This chapter is based on the publication: A. Bouakaz, J. Borsboom and N. de Jong. New contrast imaging method using double frequency exposure. *2004 IEEE Ultrason. Sympos. Proc.*, in press.

6.1 INTRODUCTION

Ultrasound contrast agents are indicated and routinely used for left ventricular opacification (LVO) and for enhanced endocardial border delineation[20]. In the past, much research effort has been put into the development of new detection methods to optimise the image quality in these application areas. This research has lead to imaging methods such as pulse inversion imaging, power modulation imaging and power doppler that have resulted in significant improvements in image quality. Another application area for ultrasound contrast agent is the assessment of mycardial perfusion. In this area, substantial research effort is still undertaken. The recently developed contrast imaging methods such as pulse inversion and power modulation that are now effectively used for LVO have shown limited success in detecting myocardial perfusion during echocardiographic examinations with 'difficult-to-image' patients. Therefore, new imaging methods are investigated that exploit the unique acoustic properties of gas-filled microbubbles[4, 39]. The ultimate perfusion imaging technique should deliver maximal suppression of the strong, linear or non-linear tissue echoes while optimising the strength of the bubble echoes. The discrimination between non-perfused tissue and contrast-perfused tissue is usually expressed as contrast-to-tissue ratio. In this study, we present preliminary results of a new imaging technique that is capable of discriminatory detection of echoes from contrast microbubbles and suppress or eliminate echoes emanating from non-oscillating structures such as tissues. The method is based on blending of two frequency components. One frequency component induces reversible changes in the physical properties of the bubble which, subsequently, are traced by the other frequency compontent. A similar approach has been used by Deng et. al. where they used a dual frequency technique to study phenomena associated with ultrasound contrast agent bubbles[16].

6.2 METHOD

The method we describe in this paper is based on simultaneous use of two frequency components. A low frequency signal that is called the conditioning or modulating signal is used to modulate the size of the bubbles by inducing slow oscillations. These changes in size are then traced by a high frequency signal that is called the imaging or detection signal. The high frequency signal is mixed into the low frequency signal and used to interrogate the modulated bubbles or, in other terms, to image the slow oscillations of the gas bubbles as induced by the low frequency signal. The advantage of mixing the LF signal and the HF signal resides in the fact that the LF signal will reversibly alter the physical properties of the gas bubble, i.e. its size between the compression (positive cycle of the pressure signal) and expansion (negative cycle of the pressure signal) phases. With the change in size of the bubble the response of the bubble to incident ultrasound changes as well and in a non-linear way. During the two phases of the LF signal that induce the change in the size of the bubble, the HF signal is used to image the bubble. Hence, the HF signal will sense the same bubble at two

different stages: small and large size depending on the phase of the LF signal. During the rarefaction phase of the LF signal, an enlarged bubble is insonified with the high frequency signal while during the compression phase of the LF signal, a smaller bubble is insonified with the high frequency signal. Consequently, the response of the bubble to the HF imaging signal will differ from the positive to the negative cycles of the LF conditioning signal. We should stress here that the non-linear change in response that is due to the change in bubble size is critically important. The response of a 'linear bubble' would simply be the summation of the LF and HF responses. This implies that the change in size as induced by the LF excitation would not change the response to the HF excitation. When non-oscillating scatterers such as tissue are present, the response will be hardly different in both phases of the conditioning LF signal since these scatterers do not oscillate and, hence, undergo a change in physical properties. This finding will increase the distinction between gas bubbles and tissue thus improving the contrast-to-tissue ratio.

6.3 SIMULATIONS

Simulations were carried out using the modified Herring equation[32, 44]. The purpose of the simulations was to investigate the principles of the method. A free air bubble of 1.2 μm radius was insonified with a double frequency signal consisting of 1 cycle at 0.5 MHz and 7 cycles at 3.5 MHz. The high frequency signal covered thus the whole length of the low frequency signal. The acoustic pressures were 30 kPa and 180 kPa for the low frequency and high frequency signals respectively.

6.4 EXPERIMENTS

To evaluate the usefulness and sensitivity of the double-frequency insonification in differentiating between gas bubbles and tissue, optical observations were carried out with the Brandaris-128 camera system[10]. The Brandaris-128 is a high speed digital camera capable of acquiring in a single run 128 frames at a speed of 25 million frames per second. To interrogate the bubbles at 2 different frequencies, two broadband transducers were used with center frequencies of 0.5 MHz and 3.5 MHz. The transducers were mounted in a Plexiglass® container and positioned such that their focal distances coincided at a depth of 75 mm. The acoustic pressures corresponded to mechanical indices of 0.2 at 0.5 MHz and less than 0.1 at 3.5 MHz. In this experiment, the optical observations were carried out at a frame rate of 14 million frames per second. At this frame rate 128 successive frames were recorded. Sonovue contrast agent was used in the experiments.In this study, we show an example of a bubble of 4 μm diameter oscillating under the effects of both 0.5 and 3.5 MHz signals.

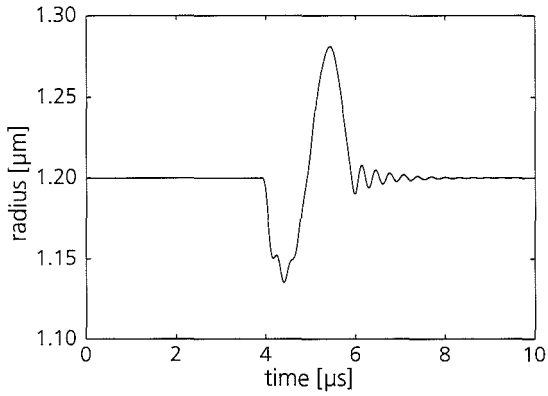

Figure 6.1: Radius-time curve of a 1.2 μm free air bubble insonated with a 0.5 MHz pulse at 15 kPa peak pressure.

6.5 RESULTS

Figure 6.1 shows the simulated radius expansion of 1.2 μm free air bubble when insonified with the low frequency signal alone (0.5 MHz). We see that the bubble under these interrogation settings compresses to almost 1.14 μm and then expands to almost 1.28 μm. Therefore the bubble size changes from 1.14 μm to 1.28 μm when switching from rarefaction to compression phases. Therefore when the 3.5 MHz high frequency signal is associated with the 0.5 MHz signal, it will sense the same bubble but at two different sizes.

Figure 6.2 displays the scattered echoes from 1.14 μm (—) and 1.28 μm (---) bubbles at the fundamental frequency after insonification with a 3.5 MHz signal. The figure demonstrates a significant difference between the two echoes where the small bubble clearly scatters more energy than the large bubble. In this case, the difference is 3.9 dB. Figure 6.3 shows the responses of the two bubbles at the second harmonic frequency. Since the small bubble is closer to the resonance size at the excitation frequency (3.5 MHz), its scattering capabilities at the second harmonic frequency are much higher than the large bubble. The difference in scattered power is 14.5 dB. These curves illustrate that a low frequency signal can be used to modify the size of a gas bubble, and then detect these size changes with a high frequency signal.

Figure 6.4 shows the results obtained with the high-speed camera. It displays the diameter-time curve of a 4 μm Sonovue microbubble irradiated with the double frequency signal. We can see that the bubble diameter consists of a high frequency signal (3.5 MHz) modulated with a low frequency signal (0.5 MHz). The high frequency signal is mainly apparent during bubble compression while it is hardly seen in the compression phase.

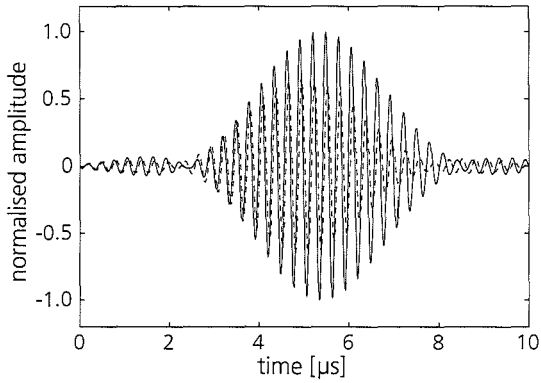

Figure 6.2: Simulated echoes at fundamental frequency of 1.14 μm (—) and 1.28 μm (---) bubbles after excitation with a 3.5 MHz signal.

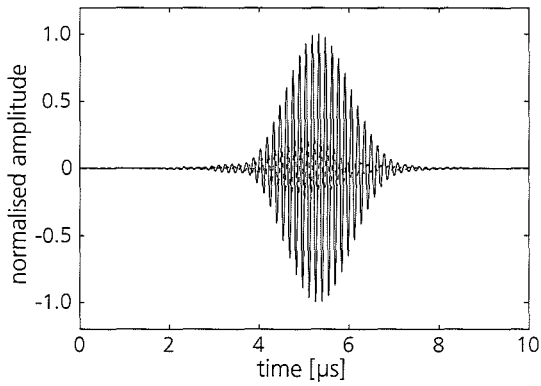

Figure 6.3: Simulated echoes at second harmonic frequency of 1.14 μm (—) and 1.28 μm (---) bubbles after excitation with a 3.5 MHz signal.

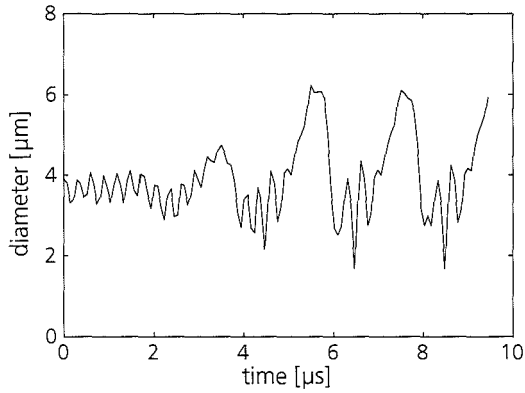

Figure 6.4: Diameter-time curve of a Sonovue microbubble insonified with a double frequency signal of 0.5 MHz and 3.5 MHz.

Figure 6.5 shows the diameter time curves at 3.5 MHz (—) and 0.5 MHz (---) after filtering. We can observe that up to 3 μs, the 0.5 MHz signal amplitude is low and thus the bubble response at 3.5 MHz is almost constant between compression and expansion phases. After 3 μs, the amplitude of the 0.5 MHz signal increases making the bubble oscillations more evident. The bubble diameter compresses to about 3 μm and expands up to 6 μm. During these oscillations, the 3.5 MHz imaging signal interrogates thus the same bubble but that has a variable size. In this case we clearly appreciate that the response at 3.5 MHz shows clear differences between compression and expansion phases. During compression (smaller bubble), the bubble's response at 3.5 MHz is much larger than its response during expansion phase. During expansion phase, the bubble becomes larger and thus far away from the resonance size, reducing by that its total response. The decorrelation between the compression and expansion phases of the LF signal in the 3.5 MHz bubble response is significantly high to be used as a parameter to detect gas bubbles and discriminate between oscillating structures (contrast bubbles) and non-oscillating structures (tissues).

6.6 CONCLUSIONS

The theoretical and experimental results demonstrate the principles and feasibility of this approach in improving the discrimination between microbubble echoes and tissue echoes. Future work consists of evaluating acoustically the performances of such a method on a cloud of contrast microbubbles and comparison with current contrast imaging methods such as pulse inversion or power modulation.

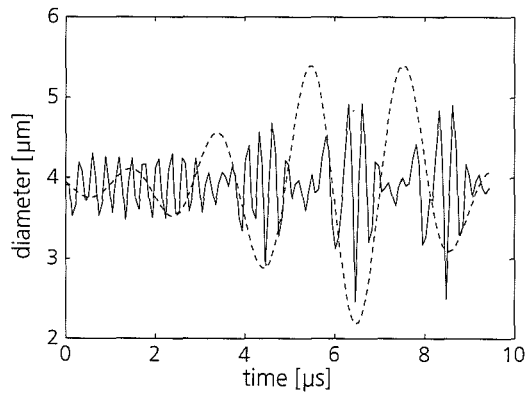

Figure 6.5: Diameter-time curves filtered around 0.5 MHz (---) and 3.5 MHz (—).

7 PULSE SUBTRACTION IMAGING METHOD FOR ULTRASOUND CONTRAST AGENT DETECTION

ABSTRACT

Detection of contrast agents in perfused tissue has been an important research topic for many years. Currently available methods are based on the high non-linear scattering of a contrast agent bubble or destruction of the agent. Among the best known methods are harmonic imaging, power modulation and pulse inversion. These techniques use a spectral filtering approach to extract that part of the spectrum in which the received signal shows the largest difference between tissue and contrast agent. The approach introduced in this paper deviates from a spectral filtering approach in that it uses differences in system behaviour between tissue and bubbles to detect the contrast agent and suppress the tissue signal. Using two non-overlapping pulses and subtracting these from a third pulse, we selectively suppress the tissue part in the received signal by exploiting the interaction of non-linearity and absence of memory effects in tissue. Simulation results indicate tissue suppression of more than 40 dB relative to contrast agent in fundamental and second harmonic. In-vitro measurements are in agreement with the simulation resuls showing suppression of 20 dB for fundamental and 15 dB for second harmonic.

This chapter is based on the patent application: J.M.G. Borsboom, A. Bouakaz, and N. de Jong. Techniques for improving ultrasound contrast ratio.

7.1 INTRODUCTION

Ultrasound contrast agent in the form of small gas bubbles (average diameter of 3 μm) were introduced to improve the image quality. The gas bubbles are infused into the region of interest to increase the backscattered echoes from the desired organs. They are currently utilized mainly as tracers for the non-invasive quantification of blood flow and many of them are now approved for left ventricular opacification and for enhanced endocardial border delineation[1, 20]. To extend the utility of ultrasound contrast

for imaging, research has been actively focused in developing efficacious ultrasound contrast agents and new classes of contrast-specific imaging methods.

More stable contrast gas bubbles have been lately developed, designated as second or third generation contrast agents. They consist of shell-encapsulated core with a high molecular weight gas. The gas contained in the bubble plays the most important role in setting the lifetime and persistence of the contrast echo. The shell material controls the longevity of the bubble in addition to its linear and non-linear scattering and absorption properties. The commitment of pharmaceutical companies for new ultrasound contrast bubbles design and manufacturing was accompanied by a significant improvement in the way ultrasound imaging is performed. Specialized imaging methods were developed to preferentially detect echoes from the contrast bubbles while reducing those from other structures, such as solid tissue. This was mainly attributed to the unique acoustical signatures of gas microbubbles, which differ from signature of tissue.

One of these properties is second harmonic scattering. Second harmonic based techniques enhance the detection of contrast agent within many structures such as the cardiac chambers. They exploit the differences between the response of gas microbubbles and tissue to ultrasound irradiation. Soft tissues are known to be linear reflectors whereas contrast bubbles exhibit a nonlinear or harmonic behavior when interacting with ultrasound waves. This property has been used to selectively image contrast bubbles and is now employed in commercial systems for transthoracic imaging and termed contrast harmonic imaging[9]. Although second harmonic imaging is the first technique that gave new capabilities to contrast imaging, the differentiation between contrast and tissue, termed contrast-to-tissue ratio (CTR), is still in many situations cumbersome and contrast detection remains nowadays one of the main challenges, especially in the capillaries. The reduced CTR is mainly caused by the generation of harmonic energy from non-linear propagation effects in tissue, which hence obscures the echoes from contrast bubbles.

From the fundamental imaging used at the early age of contrast echo to second harmonic imaging, there have been several developed microbubble detection techniques. These include pulse inversion[25] and power pulse inversion[8], power modulation[7], multi-pulse release imaging[18], subharmonic imaging[17] and superharmonic imaging[4, 6]. All these detection strategies take advantage of the fact that microbubble response, and mainly its non-linear response differs from the tissue response. In this way, the specific bubble component can be separated from the tissue component. Unfortunately, in many circumstances all the contrast imaging methods still associated with various limitations that reduce their capability to discriminate tissue echoes from blood echoes, which is then translated by a reduced contrast to tissue ratio (CTR).

In this paper we introduce a new multi-pulse contrast agent imaging method. The method significantly attenuates the tissue component in a received echo signal while echoes from contrast agent pass relatively unsupressed. Using the properties of a linear and stateless system we define a three pulse sequence that cancels perfectly when

subtracted. Subsequently we show that changing the system from linear to non-linear does not change the cancellation property of the pulses. In addition, we show that in certain cases the three pulse sequence can be simplified to a two pulse sequence. The method is then applied in a simulation study which shows high suppression of echoes received from tissue and much less supression of echoes received from a contrast agent bubble. Finally, an in-vitro experiment confirms the results found in the simulations study.

7.2 BACKGROUND

Linear system theory defines a Linear Time-Invariant (LTI) system $h(t)$ as a system having the properties[37]

$$a \cdot h(x_1(t)) + b \cdot h(x_2(t)) = h(a \cdot x_1(t) + b \cdot x_2(t)) \tag{7.1}$$

and

$$\begin{aligned} x(t) &\Rightarrow y(t) \\ x(t+\tau) &\Rightarrow y(t+\tau), \end{aligned} \tag{7.2}$$

in which $x(t)$, $x_1(t)$, and $x_2(t)$ are arbitrary input signals, a and b are arbitrary scaling constants, $y(t)$ is the response of the system to the input signal $x(t)$, and τ is an arbitrary time delay. Equation 7.1 defines linearity and is well known. Equation 7.2 defines time-invariance which states that a time shift on an input signal does not change the response of a system except for an equal time shift in the output signal. Real-life systems are, in addition, necessarily causal which implies that the output of such a system can not depend on input in the future. This can be expressed as

$$y(\tau) = h[x(t)] \quad \text{with} \quad t \leq \tau, \tag{7.3}$$

in which $h[\ ]$ indicates what values the system $h(t)$ uses to determine its output. Another property in system theory is the notion of 'state' or 'memory' in the system. The output of state- or memoryless systems depends only on the current input and not on any input in the past. A memoryless system can hence be expressed as

$$y(\tau) = h[x(t)] \quad \text{with} \quad t = \tau. \tag{7.4}$$

An example of a stateless and causal LTI-system is an electrical resistor network. The notions of linearity and state in system theory are orthogonal concepts and therefore every combination of the two is possible.

In ultrasound, the complete imaging chain can be classified by these concepts as well. In the early days, the imaging system for tissue was considered to be a linear and time-variant system; linear because transducer and tissue scattering were considered linear and time-variant because of movement in the imaged region, for example in the

case of imaging the human heart. More recently, harmonic imaging was introduced, which necessitated reclassification of an imaging system as a non-linear, time-variant system. Although the transducer was still considered linear, the medium was found to produce harmonics at higher ultrasound pressures and hence to be non-linear. Additionally, due to the high Pulse Repetition Frequencies (PRF's) currently used, the imaging system has essentially become time-invariant on the inter-pulse time-scale which is exploited in multi-pulse techniques like pulse inversion and power modulation. As for state in the imaging system, it is clear that the imaging chain contains state information, which is most apparent from the delay between transmission of the pulse and reception of the response. The highly damped, large bandwidth transducers currently in use are well able to follow the electrical signal applied to them without showing much resonant behaviour and hence the state information they contain is limited. Linear propagation is stateful as the medium contains the propagating ultrasound pulse and delays the response for the time it travels from the transducer to a scatterer and back. However, this statefulness only amounts to a delay on the input signal and is easily discarded by working in retarded time $\tau = t - \frac{z}{c_0}$, in which z is the distance the excitation pulse has travelled and c_0 is the speed of sound in the medium. From the KZK-equation, that models non-linear propagation in tissue, we can deduce that the diffraction component in this equation is the only component that introduces state. Diffraction, however, is an effect that is not limited to non-linear propagation and fully dependent on transducer geometry. Therefore, it is known in advance and can be taken into account when designing the transducer and the excitation. The non-linearity and the absorption components of the KZK-equation are stateless as their effect only depends on the instantaneous value of the pressure in the medium. In summary, ultrasound imaging of tissue behaves on inter-pulse time-scale as a non-linear and time-invariant system without any state in tissue except for a propagation delay.

The introduction of ultrasound contrast agents (UCA's) into the blood stream and tissue adds a new component to the imaging chain. UCA can be classified as a non-linear and stateful system, either time-invariant or time-variant on inter-pulse time-scale. Non-linearity of a contrast agent bubble has been early recognised and used in various non-linear imaging techniques. The statefulness is easily appreciated from its resonant behaviour; a clear peak is visible in the response of a single contrast agent bubble when insonified at resonance frequency. Time-invariance or time-variance of a bubble system is dependent on the excitation pressure that is used to insonify the bubble. High excitation pressures change or destroy the bubble and hence the system becomes time-variant. If the pressure is low enough not to destroy or change the bubble at each firing, the system becomes time-invariant on inter-pulse time-scale.

Comparing the system theoretic classification of tissue and contrast agent in table 7.1, we see that at low pressures both are time-invariant, tissue is linear while contrast is non-linear, and finally that tissue is stateless while contrast is stateful. The difference in linearity between tissue and contrast is exploited in techniques that are based on differences in non-linear responses, for example harmonic imaging, pulse

Table 7.1: System theoretic behaviour of tissue and contrast agent bubbles

	tissue	contrast agent
low pressure	• linear • time-invariant • stateless	• non-linear • time-invariant • stateful
high pressure	• non-linear • time-invariant • stateless	• non-linear • time-variant • stateful

inversion and power modulation. These techniques use a signal processing approach to selectively extract the harmonic part from the received signal and hence detect the presence of contrast agent in tissue. Currently, no techniques are known to the authors that are based on statefulness to detect the presence of contrast agent bubbles in tissue. At high pressures, both tissue and bubble become non-linear. This property, therefore, cannot be used anymore at high pressures to differentiate between bubbles and tissue. However, at higher pressures which causes the bubble to change or even to be destroyed, contrast agent becomes time-variant. This property is used in techniques like power Doppler and release burst imaging which use correlation based techniques to track the change in signature in the received signal from the contrast agent after a high power excitation pulse to disrupt the contrast agent. As with low power excitation, there are currently no known techniques that exploit the difference in statefulness between tissue and contrast agent.

An important goal in contrast agent imaging has been the detection of contrast agent in perfused tissue. Currently most techniques are either based on the high non-linearity of a contrast agent bubble relative to tissue or the disruptability of the bubble. In both methods, however, tradeoffs have to be made when implemented in current ultrasound machinery. Techniques based on non-linearity suffer from the non-linearity coming from tissue. As the non-linearity from tissue is confounded with the non-linearity from the contrast agent, it is very hard to untangle both signals and hence the quality of the image deteriorates from these contaminating tissue harmonics. In addition, the bandwidth of the transducer has to be divided to fit both transmission and reception bandwidth. The techniques based on disruption of the bubble cannot be used at high PRF's. As at each firing bubbles are destroyed, high PRF's would destroy all the bubbles before new ones arrive with the blood stream leaving no contrast agent in the imaged region. This effect severely limits the PRF and hence the image frame rate.

In this paper we propose a new signal processing approach that is based on the interaction between the non-linearity of a contrast agent bubble and its statefulness to selectively identify and suppress the response of tissue and improve the contrast to

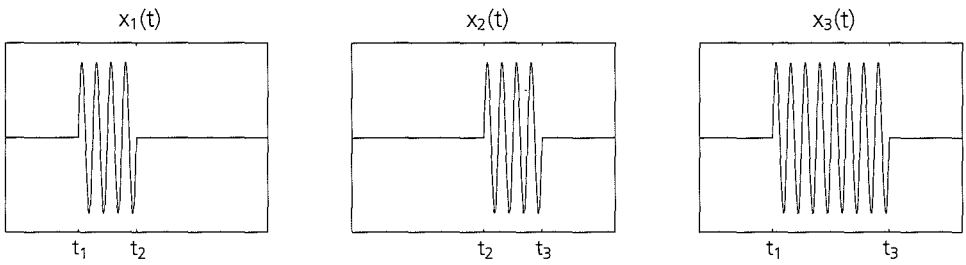

Figure 7.1: Three pulse combination that cancels perfectly when x_1 and x_2 are subtracted from x_3.

tissue ratio (CTR). Although the technique uses non-linearity, it does not need to record harmonics in the reflected signal which implies that transducers can be used at their optimal bandwidth. As it is mainly a low excitation pressure technique it does not disrupt the bubbles and can be used at high PRF.

7.3 THEORY

BASIC EQUATIONS

Based on the response expected for a linear system as defined in Eq. 7.1, we define three excitation signals $x_1(t)$, $x_2(t)$, and $x_3(t)$ such that for $t_1 < t_2 < t_3$

$$\begin{aligned} x_3(t) &= x_1(t) + x_2(t) && \forall \quad t \\ x_1(t) &= 0 && \forall \quad t \leq t_1 \ \wedge \ t > t_2 \\ x_2(t) &= 0 && \forall \quad t \leq t_2 \ \wedge \ t > t_3 \\ x_3(t) &= 0 && \forall \quad t \leq t_1 \ \wedge \ t > t_3. \end{aligned} \tag{7.5}$$

Figure 7.1 shows an example of such signals. Using Eq. 7.1 it is clear that the response $y_3(t)$ of a linear system $h(t)$ to the input $x_3(t)$ equals the summed response of the system to the inputs signals $x_1(t)$ and $x_2(t)$, or

$$\begin{aligned} y_3(t) - y_1(t) - y_2(t) &= 0 && \forall \quad t \\ y_1(t) &= h(x_1(t)) \\ y_2(t) &= h(x_2(t)) \\ y_3(t) &= h(x_3(t)). \end{aligned} \tag{7.6}$$

For a non-linear system this is not necessarily the case as Eq. 7.1 is not valid for non-linear systems. However, for a memoryless non-linear system for which $y(t) = 0$ if $x(t) = 0$, Eq. 7.6 is still valid since

$$\begin{aligned} x_3(t) &= x_1(t) \quad \forall \quad t_1 < t \leq t_2 \\ x_3(t) &= x_2(t) \quad \forall \quad t_2 < t \leq t_3 \\ x_3(t) &= 0 \quad \forall \quad t \leq t_1 \ \wedge \ t > t_3. \end{aligned} \tag{7.7}$$

Using Eq. 7.4 on these inputs for a memoryless non-linear system $n(t)$ it is clear that

$$\begin{aligned} y_3(t) &= n(x_3(t)) = n(x_1(t)) = y_1(t) \quad \forall \quad t_1 < t \leq t_2 \\ y_3(t) &= n(x_3(t)) = n(x_2(t)) = y_2(t) \quad \forall \quad t_2 < t \leq t_3 \\ y_3(t) &= 0 \quad \forall \quad t \leq t_1 \ \wedge \ t > t_3. \end{aligned} \tag{7.8}$$

Concatenating time intervals and noting that we assumed $y(t) = 0$ if $x(t) = 0$ it is proven that Eq. 7.6 is valid for non-linear memoryless systems when using input signals according to Eq. 7.5.

ULTRASOUND APPLICATION

Applying this approach to ultrasound imaging with contrast agents the power of this technique becomes clear. Our aim is to suppress the signal coming from tissue to increase the relative contribution of the contrast agent signal and hence increase the CTR. As is clear from table 7.1, tissue reacts either linearly or non-linearly depending on the applied ultrasound pressure. Suppression of the tissue signal in the linear case is possible by using any combination of three excitation signals so that $x_3(t) = x_1(t) + x_2(t)$ is true. For higher ultrasound pressures, when tissue starts to react non-linearly, this approach does not necessarily obtain full cancellation of the tissue signal anymore. However, as tissue remains stateless in both excitation conditions, the signal from tissue can be cancelled by using a pulse sequence as defined in Eq. 7.5. Contrast agents react differently. A contrast agent bubble is non-linear for both low and high power excitations and, unlike tissue, is statefull. This implies that Eqs. 7.6 and 7.7 do not hold for reflections coming from contrast agent bubbles. Therefore, full cancellation of contrast agent signal will not occur and a residual contrast agent signal will remain. When this residual signal is large enough to be detected, an increase in CTR can be obtained without destroying the bubble or using harmonic components from the response.

A physical explanation of the residual signal is an interaction between the non-linearity and the statefulness of the contrast agent bubble. Signals from linear systems always cancel, irrespective of any state in the system; for non-linear systems, the signals only cancel when the system is stateless. For a stateful system, the output at time t does not only depend on the input at time t, but also on the input before t. In Fig. 7.1, we see that the last half of signal $x_3(t)$ equals $x_2(t)$. In $x_3(t)$, however, there is a signal before that last half, that is absent in $x_2(t)$. When a stateless system responds to $x_3(t)$ as input, the last half of the response will be equal to the response from $x_2(t)$ as it does

not matter what has happened before current time for a stateless system. When the system is stateful, it does matter what has happened before and hence the output for the last half will differ. Signal $x_1(t)$ is used to calculate the response of the first half of $x_3(t)$, which for both a stateless and stateful system should match perfectly as all real-life systems are causal and cannot look into the future.

When implementing this technique into real hardware a few issues are encountered. Firstly, transducers have finite bandwidth and hence cannot exactly reproduce the non-overlapping waveforms. This issue only becomes important when imaging tissue in non-linear regime, i.e. at high ultrasound pressures. In linear regime, the waveforms still fully cancel as only the linearity property is used and the distortions introduced at the front and the back of the waveform by the finite bandwidth of the transducer fully cancel. In non-linear regime, some residual signal is expected from the tissue which will confound with the residual signal from the contrast agent and decrease the obtained CTR in the image. However, as this is a fixed and fully transducer dependent effect, it can be compensated for in the pulser to minimise the overlap in the signals to limited transducer bandwidth. Secondly, when using a pulse sequence as defined in Fig. 7.1, a pulsing scheme which transmits only two pulses will suffice. As the only difference between $x_1(t)$ and $x_2(t)$ is a time delay of exactly four cycles and we consider the system to be time-invariant, we can use $x_1(t)$ to generate both $y_1(t)$ and $y_2(t)$ by delaying $y_1(t)$ four cycles to obtain $y_2(t)$. Using fewer transmitted pulses will improve frame rate and make it easier to compare this technique with pulse-inversion and power-modulation which are both based on two transmit firings.

7.4 METHOD

To evaluate the feasibility of the new imaging approach we performed simulations of non-linear propagation and a single contrast agent bubble. Additionally, the simulation results were validated with in vitro measurements of a phantom and a low concentration dilution of an experimental contrast agent. For the simulations and the measurements an excitation sequence was defined which is shown in Fig. 7.2. The sequence consists of an eight cycle burst at 2 MHz, followed by two four cycle bursts at 2 MHz. All bursts have equal amplitude and are spaced T_{PRF} apart with an additional delay of four cycles (T_4) for the last four cycle burst. A two bursts excitation sequence can easily be derived from the three bursts excitation sequence by omitting the last four cycle burst. After recording the responses to the three excitation bursts, a processing step is needed to obtain the tissue suppression result. The processing step for the three burst scheme is depicted in Fig. 7.3(a). The two four cycle bursts are appropriately delayed and subtracted from the eight cycle burst. For the two bursts excitation schema, the processing is depicted in Fig. 7.3(b). Here, the single four cycle burst is delayed for four cycles (T_4) and both the original four cycle burst and the delayed version are subtracted from the eight cycle burst.

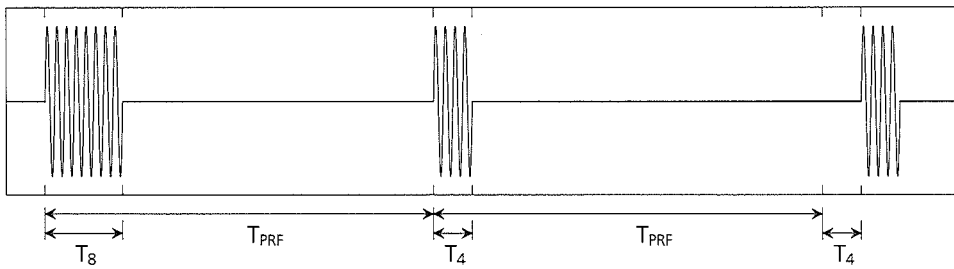

Figure 7.2: Excitation sequence with cancellation property that was used in simulation study and in-vitro measurements.

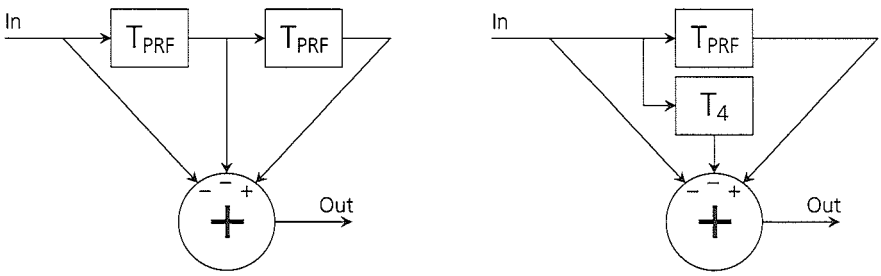

Figure 7.3: Diagram of processing steps for the three burst scheme (a) or two burst scheme (b).

SIMULATIONS

The effects of non-linear propagation in tissue were simulated by solving the KZK-equation[26]. A computer program was written in Matlab (The Mathworks, Inc., Natick, MA, USA) and C to solve the parabolic wave equation in time domain for arbitrary excitations. The program was used to calculate the on-axis response at the focus of a 25 mm diameter focussed single element transducer. The focal depth of the transducer was 75 mm; the coefficient of absorption and the coefficient of non-linearity ($\frac{B}{A}$) were set $4.3 \cdot 10^{-6}$ $\frac{m^2}{s}$ and 2.5, respectively. The excitation was as defined in Fig. 7.2 and scaled to produce approximately 50 kPa, 100 kPa, 200 kPa, and 500 kPa peak pressure at the focus. At 2 MHz, these pressures correspond to mechanical indices (MI's) of 0.035, 0.07, 0.14 and 0.35 of which the first two are in the range used in non-destructive contrast agent imaging. The pressure waveforms resulting from the simulation were appropriately delayed and subtracted according to Fig. 7.3(a) to obtain the suppressed tissue signal.

The response of a single contrast agent bubble was calculated from a modified RPNNP differential equation[15], named after its developers Rayleigh, Plesset, Noltingk, Neppiras and Poritski, using Simulink and Matlab. A single contrast agent bubble with 2.75 μm radius and a resonance frequency of 2.0 MHz was excited with the burst sequence as defined in Fig. 7.2 scaled to 10 kPa, 20 kPa, 50 kPa and 100 kPa peak pressure. By using these low peak pressures we expect to be in the range which does not disrupt the contrast agent and hence obtain simulation results valid for non-destructive contrast agent imaging. The shell property parameters were set according to the shell properties of commercially available contrast agent. The simulated pressure waveforms at some distance from the bubble were delayed and subtracted according to Fig. 7.3(a) to obtain the resulting bubble signal. Using the simulated non-linear propagation and contrast agent signals we evaluated the performance of the new approach in both time and frequency domain.

MEASUREMENTS

For evaluation of the approach, we performed an in-vitro experiment in which we processed ultrasound traces recorded from either an agar-agar, tissue mimicking phantom or a container with a low concentration of contrast agent. The phantom consisted of 3% agar-agar with 0.4% carborundum to mimic tissue scattering. The contrast agent was a 1:5000 dilution of BR-14 (Bracco Research SA, Geneva, Switzerland) in an acoustically transparent container. The experiment was performed in a water tank containing gas saturated water in which either the phantom or the contrast agent was placed at the focus of a 2.25 MHz single element broadband transducer (PZT, Ø 32 mm, 75 mm focal length (Panametrics, Waltham, MA, USA)) which was mounted at the side of the water tank. The excitation sequence was generated with an arbitrary waveform generator (LW420A, LeCroy, Chestnut Ridge, NY, USA), attenuated with a variable attenuator (355C/D, HP, Palo Alto, CA, USA), and amplified

by a 50 dB linear power amplifier (2100L, ENI, Rochester, USA). To keep bubble disruption to a minimum, the maximum MI was 0.1. The echo signal was recorded with an 8-bit digital oscilloscope (9400A, LeCroy, Chestnut Ridge, NY, USA) and processed off-line on an IBM-compatible PC. To increase the accuracy of the timing and to obtain a measurement of the decorrelation due to bubble movement, the excitation sequence was slightly modified by removing the T_4 delay of the last four cycle burst. The processing scheme used was the two burst scheme depicted in Fig. 7.3(b). T_{PRF} was set to 160 μs. To lower the noise level in the phantom measurements, we averaged 1000 traces. As contrast agent bubbles are moving around and hence the traces are not time-invariant, this was not appropriate for the contrast agent traces and non-averaged traces were used for processing. Therefore, the noise level in the contrast agent measurements is higher than the noise level in the phantom measurements.

7.5 RESULTS

The results from the non-linear and contrast agent bubble simulations are depicted in Figs. 7.4 and 7.5. Both figures show in columns the signals that occur at several points in the processing chain for the previously defined peak pressures. The upper three rows show the results from the Matlab simulation programs with each graph normalised to the peak pressure at the top of the column in which it resides and aligned in time for the subtraction of the two four cycle bursts from the eight cycle burst. It is clear that the responses from the two four cycle bursts differ only by a time shift. The fourth row shows the result from the subtraction. Although both for non-linear propagation and for a contrast agent bubble the amplitude of the residual signal increases for increasing peak pressure, the scaling of the figures is made different for visibility of the residual signal. For non-linear propagation in Fig. 7.4 the vertical axis is scaled to 1/10 of the vertical scale of the graphs above; for the contrast agent bubble in Fig. 7.5 the vertical axis is scaled to only 1/2 of the vertical scale above. Another clear difference between the residual signals is their length in time and periodicity. The main part of the residual signal from non-linear propagation is very bounded in time; it consist of a single cycle that, in addition, has a frequency that is much higher than the frequency of the excitation. On the other hand, the contrast bubble residual signal is much longer in time and clearly shows a fundamental frequency that is equal to the frequency of the excitation. Finally, the last row shows the Fourier transforms of the four cycle response from the second row and the residual signal from the fourth row. Additionally, the graphs are not normalised and hence are comparable between columns. For non-linear propagation we see large suppression of the non-linear propagation signal. At the fundamental at 2 MHz the amount of suppression ranges from approximately 80 dB for the 50 kPa signal to 50 dB for the 500 kPa signal. In addition, the frequency spectrum of the residual signal is almost flat and shows no clear fundamental and harmonic frequency components. For the contrast agent bubble we see suppression of the reflected signal as well, but to a much lesser extend.

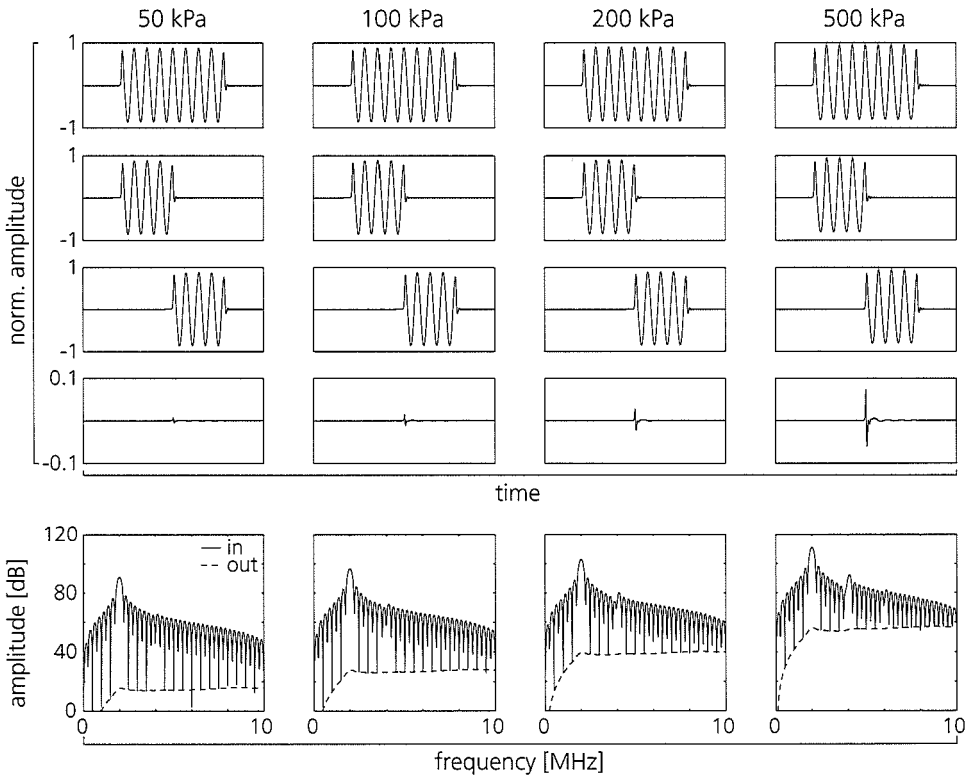

Figure 7.4: Simulated pressure-time curves for non-linear propagation with KZK-equation at several excitation pressures. The top three rows depict, in time domian, the signals before processing, the fourth row, in time domain, the resulting signal after processing, and the bottom row the signals before (—) and after (---) processing, in frequency domain.

We the fundamental is suppressed approximately 40 dB at 10 kPa excitation and 20 dB at 100 kPa excitation. At the second harmonic, the lack of suppression is more even clear as in all cases the suppression is only a few dB's. In addition, the residual signal shows the fundamental frequency component and the higher harmonics.

The results from the in-vitro experiments are in accordance with the simulation results and are shown in Fig. 7.6. The two columns show the signals as obtained from the tissue mimicking phantom and the contrast agent dilution. The top row shows the received signal from the four cycle burst, the middle row the residual signal after processing and the bottom row the Fourier transforms of the signals above. The suppression for the phantom is clearly seen in the time signal which contains mainly noise after processing as well as in the Fourier transform graph which nicely shows the suppression of the received signal in the bandwidth of the transducer. At the fundamental

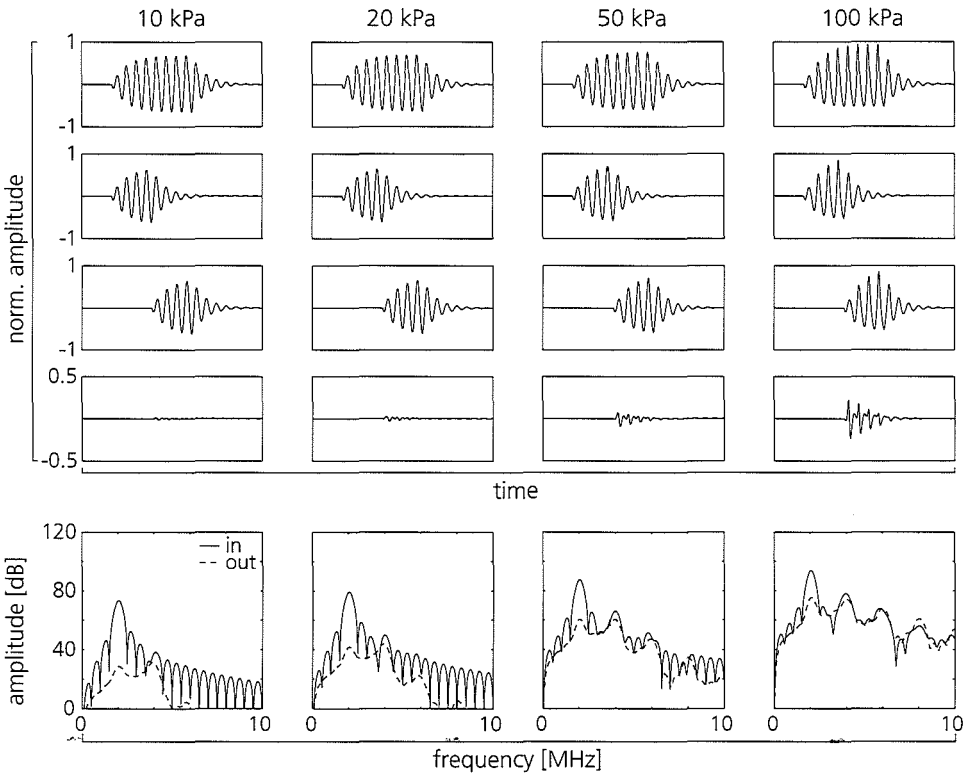

Figure 7.5: Simulated pressure-time curves for a single contrast agent bubble using a modified RPNNP-equation at several excitation pressures. The top three rows depict, in time domian, the signals before processing, the fourth row, in time domain, the resulting signal after processing, and the bottom row the signals before (—) and after (---) processing, in frequency domain.

and second harmonic we see suppression of approximately 25 dB and 15 dB respectively. Comparing this with the received signal from the contrast agent dilution, we see a slight decrease in average amplitude in the time signal after processing. In the Fourier transform graph a slight suppression is visible around the fundamental; at other frequencies the curves overlap.

7.6 DISCUSSION

Detection of contrast agent in perfused tissue has been an important research topic for many years. The methods that are currently available are either based on the high non-linear scattering of a contrast agent bubble or destruction of the contrast agent. The most important representatives of the first method are harmonic imaging, power modulation and pulse inversion. All three techniques use a spectral filtering approach to extract that part of the spectrum in which the received signal shows the largest difference between tissue and contrast agent. A drawback of these techniques is that the transducer bandwidth is implicitly or explicitly divided into a transmission sub-band and a reception sub-band and therefore not optimally used. Differences in system theoretic behaviour of non-linear propagation and contrast agent are not used with these techniques. The maximum obtainable CTR is hence limited by differences in non-linearity. The approach introduced in this paper uses the difference in system behaviour between tissue and bubbles to detect the contrast agent and suppress the tissue signal. The simulation results and the measurements clearly show the ability to untangle both signals and improve the contrast to tissue ratio above the CTR that is inherent in the received signal. For example, at 100 kPa simulation results show at the fundamental a suppression of 70 dB for non-linear propagation response and 18 dB for the contrast agent bubble response; an increase of approximately 52 dB in CTR after processing the signals with the new approach. For harmonics the effect are similar. For the non-linear propagation signal we find significant suppression while the bubble signal is hardly suppressed. In Fig. 7.5 we even see at 100 kPa an increase of the fourth harmonic after processing. Although the experimental setup was not optimised for this approach, we found significant suppression of the phantom signal while the contrast agent signal was hardly suppressed. Fig. 7.6 shows an approximate increase of 20 dB in CTR at the fundamental and 15 dB at the second harmonic. As we used an 8-4-4 cycle pulsing scheme in the experiments, we could check for decorrelation due to movement of the contrast agent by subtraction the responses of the two four cycle bursts. No decorrelation due to bubble movements was found and hence the residual signal can be fully subscribed to be caused by statefullness of the contrast agent.

Though the method is based on interaction between non-linearity and statefullness, the operations which implement the processing are linear operations. This implies that most techniques that are in use in ultrasound applications can still be applied. For example, pulse inversion and power modulation can still be applied; at a cost, however, of further reducing frame rate. Furthermore, as pulse inversion is already based on sub-

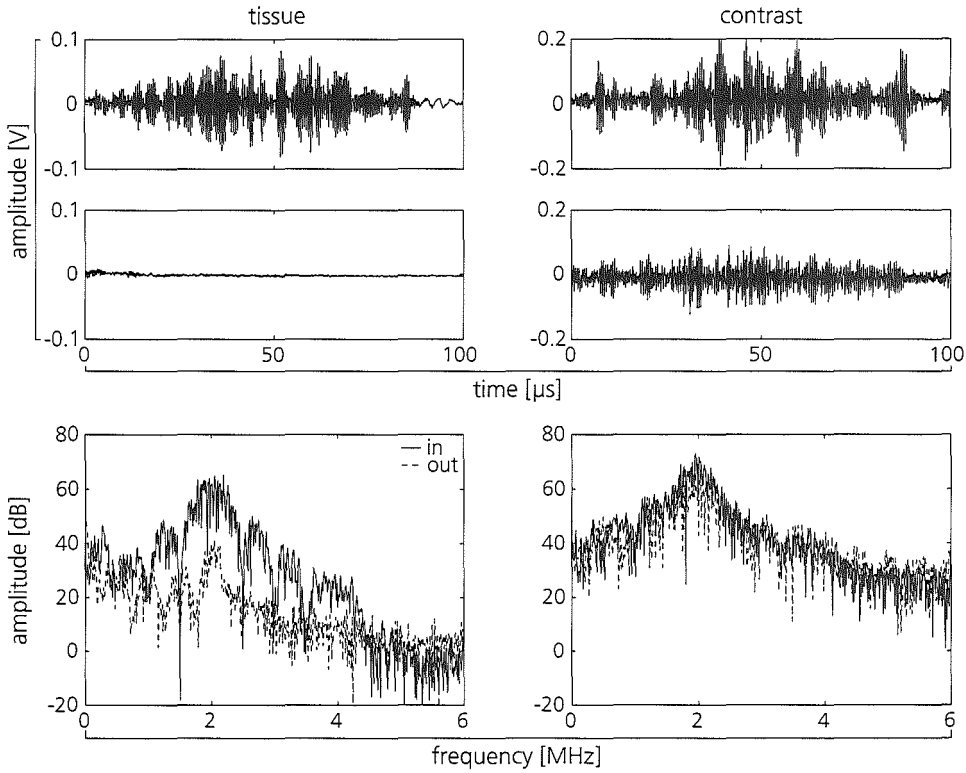

Figure 7.6: In-vitro measurements of a tissue mimicking phantom (left) and a contrast agent suspension (right). The top and bottom figures depict the measured echo signals before processing in time and frequency domain (—), respectively. The bottom figures depict the processed signals in time and frequency domain (---), showing significant suppression of the echo signal from the tissue mimicking phantom.

traction of carefully aligned traces from different firings, much of the signal processing infrastructure that is necessary to implement this technique is already available. Therefore, adding this technique to current ultrasound scanners is well possible without large investments in hardware. Although the technique is designed for non-destructive imaging, destruction of contrast agent will not immediately cancel its applicability. As destruction of the contrast agent means decorrelation of the contrast agent signals, it will show up as an increase in the residual signal after processing. However, as the decorrelation prevents full cancellation of the first four cycles of the eight cycle burst, the will be a loss in resolution in the contrast agent signal. On the other hand, as the technique is based on suppression of signals, the noise floor of the imaging system becomes the limit of suppression. In particular for low-MI imaging, further research is necessary to show if the processed contrast agent signal is visible above the noise floor. In addition, the technique is very sensitive to slight misalignments of the traces.

Extensions of this technique can be well imagined. For example, any combination of two, not necessarily equal, pulses which do not overlap in time can be used. The two pulses can differ in phase amplitude, frequency or phase or a combination of these. The third pulse is then derived by adding the former two. Another extension is the use of harmonics instead of the fundamental as described in this paper. In summary, this paper describes a new processing method based on a system theoretic view on contrast agents that highly suppresses echoes from tissue while echoes from contrast agent pass relatively unchanged. As the method is fully linear, it can be added as a front-end to existing processing schemes to give large improvements in CTR with destroying the contrast agent.

8 OVERVIEW AND CONCLUSION

8.1 GENERAL DISCUSSION

From its initial discovery, ultrasound contrast agents have been subjected to large amounts of scrutiny and research which in turn has lead to an impressive body of literature. In the early days, the only way to investigate the properties of an agent was by acoustic measurements and characterisation[12], which are inherently bulk based. Currently, we are at the point where sophisticated bubble models are available that can predict the response of a single bubble in an ultrasound field[15, 19, 11, 32]. Also, we are able to observe bubble oscillations optically with very high frame rate camera systems[10], which provides further opportunity to enhance our understanding. Using bubble models and optical observations, we can try to develop methods that use the bubble as efficiently as possible. Highly efficient use of contrast agent enables us to detect very low concentrations or even track single bubbles as they move through the capillary system. Current methods already are quite sensitive, but almost none are tailored to the specificities of contrast agent bubbles. Therefore, there is ample room for improvement and new developments in detection methods. This thesis has set out to investigate and develop new methods for detection of ultrasound contrast agent. The aim was to develop detection methods that include specific knowledge of contrast agent bubbles and, hence, improve the detectability of contrast agent.

We started the research with investigating long time-duration pulses. A bubble suspended in a liquid forms a mass-spring like system with the trapped gas being the spring and the surrounding liquid the mass. The resonant behaviour of such a system causes the bubble to react relatively slowly to an incident ultrasound pulse. In particular, when using the short time-duration pulses that are in use for imaging applications to obtain high axial resolution, the bubble is not excited to maximal radial excursion which limits the reflected energy. Moreover, we have shown that the generation of harmonic components in the response by a bubble is dependent on the radial excursion of the bubble wall. These two properties of contrast agent bubbles have lead to the investigation of chirp as excitation signal for contrast imaging and the development of a second harmonic compression technique to selectively extract and compress the second harmonic. An important reason to investigate chirp signals was their long time duration and their potential to obtain good axial resolution after compression.

An initial simulation study showed a clear advantage for chirp excitations over equal bandwidth and peak amplitude pulse excitations for bubbles around resonance. Exciting a bubble with a chirp signal instead of a regular pulse improves the second harmonic response with 3 dB relative to the fundamental which translates into an increase of 3 dB in contrast-to-tissue ratio at the second harmonic. In addition, the signal-to-noise ratio increases with approximately 10 dB due to the larger energy content of a chirp signal. Compression of simulated echoes from contrast agent bubbles showed that axial resolutions could be obtained that were comparable to resolutions obtainable with regular short pulse excitation. Range side-lobe levels, however, were dependent on the bandwidth of the exciting chirp and were shown to become prohibitively high at large bandwidths. This effect was found to be caused by the overlap between the second harmonic, and the fundamental and third harmonic for large bandwidths. As the compression filter was a simple matched filter, it could not untangle the overlap and, hence, the residual fundamental and third harmonic showed up as side lobes in the compressed signals.

Subsequent in-vitro measurements partly confirmed the results from the simulation study. An increase in the relative second harmonic level was found for chirp excitations in water tank measurements. The effect was, however, more limited than expected from the simulation study. Probably, this was caused by the low signal-to-noise ratio in the measurements and the effect of a full size distribution. Compression of second harmonic echoes from a steel reflector was found to be in agreement with simulation results in both axial resolution and side-lobe levels. Finally, imaging a flow phantom clearly indicated the strong and weak spots of the second harmonic compression technique. Imaging the tissue mimicking part of the phantom produced acceptable images that were in agreement with expected results and simulations. The part of the phantom containing contrast agent was less successfully imaged. Although the size of the flow channel in the image was sufficiently accurate, range side-lobes were clearly visible in the images. More investigation showed the second harmonic in the response from contrast agent not to be as well compressible as was to be expected from the simulation results. Compression is very sensitive to phase errors in the received signal, which will show up as range side-lobes in the compressed signal. We suspect that the bubble model we used for the simulations was not very accurate in describing the phase response of the bubble. Hence, compression performed well on simulated bubble echoes with low side-lobe levels, but failed on in-vitro measurements. We speculate that this is due to changes in the phase spectrum of the bubble echo. As a bubble is not a simple linear scatterer and will, therefore, change the phase spectrum of the incident pulse on refelction.

To check on the usability of chirps for non-destructive imaging, we investigated the difference in destructivity of chirp and pulse signal as excitation. As a chirp excitation signal contains more energy than a pulse excitation signal, it is potentially more destructive for the contrast agent. As high destructiveness makes a technique less suitable for real-time imaging purposes, we compared chirp and pulse excitation with

equal bandwidth and peak amplitude and a 10-cycle burst on destructivity. Although it was found that a chirp is more destructive than a pulse with the destructivity of the burst in between that of the chirp and the pulse, this difference was not significant at MI's below approximately 0.3. As this is well above the range that is generally considered non-destructive for contrast agent, we conclude that chirps can be used instead of equal peak amplitude pulses for contrast agent imaging without significantly more agent destruction.

Subsequently, we described a method that is based on inducing and detecting changes in the physical properties of a contrast agent bubble. As it is known that the size of a bubble is an important factor in the response of a bubble to ultrasound insonification, we tried to exploit this by using a low frequency conditioning signal to induce a change in the size of a bubble, and, simultaneously, detect the change in bubble response with a high frequency interrogation signal. Simulation results and recordings with a high speed camera system showed proof of concept and directions to use the method for a new detection method that could improve the contrast-to-tissue ratio with 10 dB.

The last line of research that is described in this thesis is the development of a new contrast agent detection methods based on the system theoretic property of state in a contrast agent bubble. As a bubble has a resonant nature, it stores energy and, hence, is stateful. By using the interaction between the statefulness and non-linearity of a contrast agent bubble and a newly developed pulse sequence we have shown that it is possible to separate the confounded response of contrast agent and tissue which is stateless. With simulations and a successful in-vitro experiment we have shown proof of concept. One of the advantages of this technique is its usability over the full bandwidth of the response as it does not imply any filtering operations. Therefore, its operating bandwidth is only limited by the bandwidth of the receiving transducer.

8.2 FUTURE

The detection methods proposed in this thesis are still not optimal which leaves ample room for improvement. Most of the detection methods currently available are based on a spectral filtering approach. Although they are performing quite well, there is not much room left for improvement as they only use inherent differences in spectral response. The newest techniques use array transducers with separate transmitting and receiving elements the separate the transmission bandwidth from the reception bandwidth. Though this may extend the range of the spectral filtering approach somewhat, it fundamentally suffers from the same problems and these transducers are expensive to manufacture. These drawbacks also apply to the chirping technique we proposed in this thesis. In addition to the problems with the compression of bubble echoes, it remains a spectral filtering technique with the same inherent limitations. More research into this direction has, therefore, to be accompanied with a more fundamental understanding of the exact response of a bubble in a sound field.

In this regard, more is to be expected from the system theoretic approach to separate bubble echoes from tissue echoes. If we are able to find a bubble specific response signature that differs from the response signature of tissue and can exploit this in a detection method, we can separate confounded echoes and detect contrast agent much better than with simple spectral filtering. The methods proposed in this thesis are only a first step in this direction, but it looks like a viable new approach to the detection problem. However, much more research is necessary and development of such methods is, again, dependent on accurate bubble models.

Although not covered by this thesis, other detection methods could be imagined that are based on controlled destruction of the agent. In general, an unencapsulated bubble is a better ultrasound scatterer than a encapsulated bubble. Current methods, use a high amplitude pulse to destroy the agent in an uncontrolled way and image the highly scattering free gas bubbles. However, as the agent is destroyed by the high powered pulse, the obtainable frame rate is limited. If we, for example, could generate free gas bubble that exist only temporarily by pushing out the gas from the shell and have the shell draw the gas back in when the bubble is no longer necessary, we can have the advantages of a free gas bubble without the limit in frame rate.

To improve the understanding of a contrast agent bubble and to develop new bubble models, the recent application of very high speed camera systems to observe a contrast agent bubble under ultrasound insonification looks very promising. Recordings made with our Brandaris-128 very high speed camera system have already shown many interesting and previously unseen bubble phenomena like compression only response, static friction and the process of gas release from a bubble. Important in this respect are the recently observed surface modes of a contrast bubble. When insonified with certain pulses a bubble does not only oscillate spherically symmetrical, but in non-symmetrical modes as well. To date, all contrast agent bubble models include only radially symmetrical oscillations. Therefore, the observation of surface modes has made it very clear that the current bubble models need to be revised to accomodate these modes. Understanding of these phenomena and their inclusion into new bubble models will, eventually, aid the development of new and better contrast agent detection methods, which is what we set out for.

BIBLIOGRAPHY

[1] H. Becher and P. N. Burns. *Handbook of contrast echocardiography: LV function and myocardial perfusion.* Springer-Verlag, Berlin, 2000.

[2] J. M. G. Borsboom, C. T. Chin, and N. de Jong. Experimental validation of a nonlinear coded excitation method for contrast agent imaging. In *IEEE Ultrason. Sympos. Proc.*, pages 1933–1936, 2002.

[3] J. M. G. Borsboom, C. T. Chin, and N. de Jong. Nonlinear coded excitation method for ultrasound contrast imaging. *Ultrasound Med. Biol.*, 29:277–284, 2003.

[4] A. Bouakaz, S. Frigstad, F. ten Cate, and N. de Jong. Super harmonic imaging: A new technique for improved contrast detection. *Ultrasound Med. Biol.*, 28:59–68, 2002.

[5] A. Bouakaz, P. J. A. Frinking, N. de Jong, and N. Bom. Noninvasive measurement of the hydrostatic pressure in a fluid-filled cavity based on the disappearence time of micrometer-sized free gas bubbles. *Ultrasound Med. Biol.*, 25:1407–1415, 1999.

[6] A. Bouakaz, B. Krenning, W. Vletter, F. ten Cate, and N. de Jong. Contrast superharmonic imaging: A feasibility study. *Ultrasound Med. Biol.*, 29:457–553, 2003.

[7] G. Brock-Fisher, M. Poland, P. Rafter, and M. Mooney. Experimental observations of the sensitivity and frequency response of the power modulation technique for contrast imaging. In F. J. ten Cate, N. de Jong, and D. O. Cosgrove, editors, *Fifth Heart Centre European Symposium on Ultrasound Contrast Imaging*, pages 1–77, Rotterdam, 2000.

[8] P. Burns. Instrumentation for contrast echocardiography. *Echocardiography*, 19:241–258, 2002.

[9] P. N. Burns, J. E. Powers, and T. Fritzsch. Harmonic imaging: A new imaging and Doppler method for contrast enhanced ultrasound. *Radiology*, 185:142, 1992.

[10] C. T. Chin, C. Lancée, J. Borsboom, F. Mastik, M. Frijlink, N. de Jong, M. Versluis, and D. Lohse. Brandaris 128: A 25 million frames per second digital camera with 128 highly sensitive frames. *Rev. Sci. Instrum.*, 74:5026–5034, 2003.

[11] C. C. Church. The effects of an elastic solid surface layer on the radial pulsations of gas bubbles. *J. Acoust. Soc. Am.*, 97:1510–1521, 1995.

[12] N. de Jong. *Acoustic properties of ultrasound contrast agents.* PhD thesis, Erasmus University Rotterdam, 1993.

[13] N. de Jong. Mechanical index. *Eur. J. Echocard.*, 3:73, 2002.

[14] N. de Jong, A. Bouakaz, and P. Frinking. Basic acoustic properties of microbubbles. *Echocardiography*, 19:220–240, 2002.

[15] N. de Jong, R. Cornet, and C. T. Lancée. Higher harmonics of vibrating gas filled microspheres. Part one: Simulations. *Ultrasonics*, 32:447–453, 1994.

[16] C. Deng, F. Lizzi, A. Kalisz, A. Rosado, R. Silverman, and D. Coleman. Study of ultrasonic contrast agents using a dual frequency band technique. *Ultrasound Med. Biol.*, 26:819–831, 2000.

[17] F. Forsberg, W. T. Shi, and B. B. Goldberg. Subharmonic imaging of contrast agents. *Ultrasonics*, 38:93–98, 2000.

[18] P. J. A. Frinking, E. I. Céspedes, J. Kirkhorn, H. Torp, and N. de Jong. A novel ultrasound contrast imaging approach based on the combination of multiple imaging pulses and a separate release burst. *IEEE Trans. Ultrason. Ferroelec. Freq. Contr.*, 48:643–651, 2001.

[19] P. J. A. Frinking and N. de Jong. Acoustic modelling of shell-encapsulated gas bubbles. *Ultrasound Med. Biol.*, 24:523–533, 1998.

[20] B. B. Goldberg, J. S. Raichlen, and F. Forsberg, editors. *Ultrasound contrast agents: Basic principles and clinical applications.* Martin Duntiz, London, second edition, 2001.

[21] J.-M. Gorce, M. Arditti, and M. Schneider. Influence of bubble size distribution on the echogenicity of ultrasound contrast agents: A study of SonoVue™. *Invest. Radiol.*, 35(11):661–671, 2000.

[22] R. Gramiak and P. M. Shah. Echocardiography og the aortic root. *Inverst. Radiol.*, 3:356–366, 1968.

[23] R. Gramiak, P. M. Shah, and D. H. Kramer. Ultrasound cardiography contrast studies in anatomy and fuction. *Radiology*, 92:939–948, 1969.

[24] S. Hilgenfeldt, D. Lohse, and M. Zomack. Sound scattering and localized heat deposition of pulse-driven microbubbles. *J. Acoust. Soc. Am.*, 107:3530–3539, 2000.

[25] D. Hope Simpson, C. T. Chin, and P. N. Burns. Pulse inversion Doppler: A new method for detecting nonlinear echoes from microbubble contrast agents. *IEEE Trans. Ultrason. Ferroelect. Freq. Contr.*, 46(2):372–382, 1999.

[26] Y. Lee and M. F. Hamilton. Time-domain modelling of pulsed finite-amplitude sound beams. *J. Acoust. Soc. Am.*, 97(2):906–917, 1995.

[27] T. G. Leighton. *The acoustic bubble.* Academic Press, New York, 1994.

[28] H. Medwin. Counting bubbles acoustically: A review. *Ultrasonics*, 15:7–13, 1977.

[29] D. L. Miller. Ultrasonic detection of resonant cavitation bubbles in a flow tube by their second-harmonic emissions. *Ultrasonics*, 19:217–224, 1981.

[30] T. Misaridis. *Ultrasound imaging using coded signals.* PhD thesis, Technical University of Denmark, 2001.

[31] T. X. Misaridis, K. Gammelmark, C. H. Jørgensen, N. Lindberg, A. H. Thomsen, M. H. Pedersen, and J. A. Jensen. Potential of coded excitation in medical ultrasound imaging. *Ultrasonics*, 39:183–189, 2000.

[32] K. Morgan, J. Allen, P. Dayton, J. Chomas, A. Klibanov, and K. Ferrara. Experimental and theoretical evaluation of microbubble behavior: Effect of transmitted phase and bubble size. *IEEE Trans. Ultrason. Ferroelec. Freq. Contr.*, 47:1494–1509, 2000.

[33] M. O'Donnell. Coded excitation system for improving the penetration of real-time phased-array imaging systems. *IEEE Trans. Ultrason. Ferroelec. Freq. Contr.*, 39(3):341–351, 1992.

[34] M. Postema. *Medical bubbles.* PhD thesis, University of Twente, 2004.

[35] W. H. Press, S. A. Teukolsky, W. T. Vetterling, and B. P. Flannery. *Numerical recipies in C: The art of scientific computing.* Cambridge University press, Cambridge, UK, 1993.

[36] N. A. H. K. Rao. Investigation of a pulse compression technique for medical ultrasound: A simulation study. *Med. Biol. Eng. Comput.*, 32:181–188, 1994.

[37] W. J. Rugh. *Linear system theory.* Prentice-Hall, New Jersey, second edition, 1996.

[38] B. A. Schrope and V. L. Newhouse. Second harmonic ultrasonic blood perfusion measurement. *Ultrasound Med. Biol.*, 19(7):567–579, 1993.

[39] W. T. Shi, F. Forsber, A. L. Hall, R. Y. Chiao, J. Liu, S. Miller, K. E. Thomenius, M. A. Wheatley, and B. B. Goldberg. Subharmonic imaging with microbubble contrast agents: Initial results. *Ultras. Imag.*, 21:79–94, 1999.

[40] W. T. Shi and F. Forsberg. Ultrasonic characterization of the nonlinear properties of contrast microbubbles. *Ultrasound Med. Biol.*, 26:93–104, 2000.

[41] M. I. Skolnik. *Radar handbook.* McGraw-Hill, New York, 1970.

[42] Y. Takeuchi. Chirped excitation for < -100 dB time sidelobe echo sounding. In *IEEE Ultrason. Sympos. Proc.*, pages 1309–1314, 1995.

[43] Y. Takeuchi. Coded excitation for harmonics imaging. In *IEEE Ultrason. Sympos. Proc*, pages 1433–1435, 1996.

[44] K. Vokurka. Comparison of Rayleigh's, Herring's and Gilmore's models of gas bubbles. *Acoustica*, 59:214–219, 1986.

[45] W. Wilkening. *Konzepte zur Signalverarbeitung für die kontrastmittelspecifische Ultraschallabbilung.* PhD thesis, Ruhr-Universität Bochum, 2003.

SAMENVATTING

Contrastmiddel voor ultrageluidstoepassingen werd in 1968 bij toeval ontdekt door Gramiak en Shah toen zij een kleurstof in de bloedbaan spoten en een toename van de reflectiviteit van bloed waarnamen. Sinds die tijd is er veel onderzoek gedaan naar de eigenschappen en het gedrag van deze contastmiddelen die tegenwoordig bestaan uit kleine (1-10 μm diameter) ingekapselde gasbelletjes. Dit heeft geleid tot nieuwe en betere contrastmiddelen, verfijnde modellen die het gedrag van deze belletjes proberen te beschrijven en verschillende methoden om ze zo goed mogelijk te detecteren wanneer ze in de bloedbaan aanwezig zijn. Optimaal gebruik van contrastbellen stelt ons in staat om lage concentraties contrastmiddel te detecteren of om zelfs individuele bellen te volgen. Hoewel de huidige methoden al tamelijk gevoelig zijn, zijn ze geenszins optimaal en is er dus ruimte om deze methoden te verbeteren of om nieuwe methoden te ontwikkelen. Dit proefschrift beschrijft een aantal nieuwe methoden voor contrastmiddeldetectie, waarbij er in het bijzonder gebruik is gemaak van specifieke kennis wat betreft het gedrag van een contrastbel onder ultrageluidsinsonificatie.

Het eerste deel van dit proefschrift beschrijft onderzoek naar een excitatiesignaal met een lange tijdsduur. Een contrastbel in een vloeistof gedraagt zich als een niet lineair massa-veersysteem waarin het gas in de bel de veerkracht levert en de omringende vloeistof de massa is. Zoals ieder massa-veersysteem vertoont dit systeem resonantie. Een kenmerk van resonante systemen is een traagheid in de reactie op een excitatie. Voor een contrastbel betekent dit dat de korte, breedbandige pulsen die meestal gebruikt worden voor 'imaging' te kort zijn om de bel goed in beweging te brengen. Aangezien de pulsatiebeweging van de bel de belangrijkste component in het reflecteren van het ultrageluid is, wordt er maar weinig energie weerkaatst, hetgeen de detecteerbaarheid van de bel beperkt. Hier komt nog bij dat de niet lineariteit van een contrastbel, die in een aantal detectiemethoden gebruikt wordt, afhankelijk is van de grootte van de pulsatie.

Om een bel meer te laten pulseren onderzochten we het gebruik van een chirp signaal voor het aanstralen van contrastmiddel en ontwikkelden we een niet lineaire compressietechniek. Een belangrijk voordeel van een chirp als excitatiesignaal is de lange tijdsduur en de eigenschap een goede axiale resolutie te kunnen verkrijgen na compressie. Een simulatiestudie toonde aan dat een chirp de tweede harmonische relatief ten opzichte van de 'fundamental' met 3 dB laat toenemen in vergelijking met een

Gaussiche puls met gelijke bandbreedte. Dit laat zich vertalen in een toename van 3 dB in contrast-weefselsignaalverhouding. Verder neemt de signaal-ruisverhouding met 10 dB toe bij een chirp als excitatie. De resolutie na compressie van gesimuleerde bel echo's met de niet lineaire compressietechniek is vergelijkbaar met de resolutie die verkregen wordt met puls excitatie. Bij grote bandbreedtes ontstaan door de compressie echter zijlobben die veroorzaakt worden door overlap tussen de tweede harmonische enerzijds en de 'fundamental' en derde harmonische anderzijds. In-vitro metingen bevestigden de meeste simulatieresultaten. Echter, niet lineaire compressie van echo's van klinisch contrast middel was problematisch en gaf niet het verwachte resultaat door relatie hoge waarden voor de zijlobben. Omdat chirp compressie sterk afhankelijk is van de precieze faseresponsie van het systeem, werd dit waarschijnlijk veroorzaakt door faseveranderingen in de responsie die niet goed gemodelleerd worden in het door ons gebruikte model voor contrastbellen. Hierdoor werkte de nieuwe compressietechniek wel voor de gesimuleerde responsies en niet voor de in-vitro experimenten.

Omdat een chirp per excitatie meer energie bevat dan een puls, is deze mogelijk meer destructief voor een contrastbel. Een hoge destructiviteit van een methode maakt deze minder geschikt voor 'real-time imaging' omdat na een tijdje alle bellen vernietigd zijn er er nieuwe moeten worden aangevoerd door het bloed. Om dit na te gaan, onderzochten we experimenteel de verschillen in destructiviteit tussen puls, burst en chirp. Hoewel we vonden dat een chirp inderdaad destructiever is dan een puls met de destructiviteit van de burst daar tussen in, was het verschil niet noemenswaardig voor MI's onder de 0.3 waaruit we concluderen dat voor 'real-time imaging' een chirp gebruikt kan worden in plaats van een puls voor wat betreft het vernietigen van contrastmiddel.

Vervolgens beschrijft dit proefschrift een methode die gebaseerd is op het induceren en detecteren van veranderingen in de fysieke eigenschappen van een contrast bel onder invloed van een laag frequent conditioneringssignaal. Het is bekend dat een grote contrastbel anders reageert op een excitatiesignaal dan een kleine contrastbel. De nieuwe techniek is erop gebaseerd de grootte van een contrastbel te variëren met een laagfrequent conditionerings signaal en de verandering in responsie te detecteren met een hoogfrequent interrogatiesignaal. Simulatieresultaten en opnames met een snelle camera laten zien dat dit mogelijk is en als basis kan dienen voor een gevoelige detectietechniek die 10 dB gevoeliger kan zijn dan conventionele technieken.

Een andere methods die beschreven wordt is gebaseerd op de systeemtheoretische eigenschap van toestand in een contrastbel. Omdat een contrastbel resonant is, heeft deze noodzakelijk een toestand. Dit impliceert dat de responsie van een contrastbel niet alleen afhankelijk is van de instantane druk, maar ook afhangt van het voorgaande drukverloop. Omdat weefsels niet resoneren en dus geen toestand hebben, kunnen we dit als basis gebruiken om de echo's van contrastbellen te scheiden van de echo's van weefsels. Door de contrastbel aan te stralen met een bepaalde pulssequentie kunnen we de interactie tussen deze eigenschap en de niet lineariteit van de contrastbel exploiteren en de responsies scheiden. Met simulaties en in-vitro experimenten tonen we aan dat

dit een werkende techniek is.

Tenslotte bevat dit proefschrift een overzicht en een kritische beschouwing van de beschreven methoden en een beschouwing over wat er in de toekomst aan detectiemethoden mogelijk te verwachten is.

CURRICULUM VITAE

Jerome Borsboom was born in Rotterdam, the Netherlands in 1975. He got his secondary education (gymnasium) at the Norbertuscollege in Roosendaal between 1987 and 1993.

In 1993, he started his university education at the department of electrical engineering at Delft University of Technology where he received a Master of Science degree in electrical engineering in 1998. The work for his master's thesis, entitled 'Simulation of Cylindrical Intravascular Ultrasound Transducers', was performed at the department of Experimental Echocardiography of the Erasmus MC in Rotterdam under guidance of Prof.dr. Ed Deprettere (TU-Delft) and Prof.dr.ir. Ton van der Steen (Erasmus MC). Since 1994, he has also been pursuing a degree in psychology at Leiden University. His master's thesis there will be on the subject of multilevel extensions to homogeneity analysis under guidance of Dr. Rien van der Leeden.

Since 2000, he has been employed by the Interuniversity Cardiology Institute of the Netherlands (ICIN) at the department of Experimental Echocardiography of the Erasmus MC to work towards a Ph.D. degree under supervision of Prof.dr.ir. Nico de Jong. His thesis will be on the subject of ultrasound contrast agent detection methods.